Critical behavior of a phase transition in the dynamics of interacting populations

Thibaut Arnoulx de Pirey[1] and Guy Bunin[2]

1 Centre for Condensed Matter Theory, Department of Physics, Indian Institute of Science, Bangalore 560 012, India
2 Department of Physics, Technion-Israel Institute of Technology, Haifa 32000, Israel
* thibautdepirey@gmail.com

December 5, 2024

Abstract

Many-variable differential equations with random coefficients provide powerful models for the dynamics of many interacting species in ecology. These models are known to exhibit a dynamical phase transition from a phase where population sizes reach a fixed point, to a phase where they fluctuate indefinitely. Here we provide a theory for the critical behavior close to the phase transition. We show that timescales diverge at the transition and that temporal fluctuations grow continuously upon crossing it. We further show the existence of three different universality classes, with different sets of critical exponents, highlighting the importance of the migration rate coupling the system to its surroundings.

Contents

1 Introduction

Natural ecosystems can host a stunning diversity of coexisting species. A distinctive and pervasive pattern of these high-diversity assembly is the existence of large fluctuations of population sizes, both across species at a given time [1] and across time for individual species. Indeed, at a resolution where one identifies many species belonging to a given family, dramatic fluctuations over time have been widely observed in the wild [1–3], with species alternating between states of dominance and rarity, inducing a turnover in the identity of the most abundant species. Understanding how different mechanisms contribute to these large fluctuations remains a central challenge in ecology. These fluctuations have also been observed in controlled laboratory experiments under fixed external conditions [4], highlighting the possibility that species-species interactions are a key driver of such fluctuations. From a theoretical perspective, various models of communities of interacting populations with heterogeneous interactions exhibit two dynamical phases, one in which population sizes stabilize and another in which they fluctuate [5–10]. Importantly, these fluctuations can extend over many orders of magnitude. In fact, the ratio of the largest to smallest population size may be arbitrarily large [11], with lowest populations limited only by migration of individuals from an outside species pool, if such migration exists.

In a previous work [11], we have provided a detailed analytical description of these fluctuations. We have shown that they are closely linked with the emergence of a long timescale in the problem [11–13], interpreted as the time it takes for exponential growth or decline between the smallest and largest population sizes, which may last over many generations. Here we go beyond this analysis and give a full account of the critical behavior near the transition between the two phases. We show that, in addition to the long timescales described above, there is another layer of critical slowing down: dynamics near the transition are slower. The size of the abundance fluctuations (in terms of the abundances, rather than logarithm of the abundances) are shown to grow continuously when crossing into the fluctuating phase.

The above-mentioned phase transition found in common ecological models, such as Lotka-Volterra or resource-competition models [14], is one example in a broader family: high-dimensional dynamical systems, of interest in neuroscience [15], game theory [16] and economics [17], also exhibit a phase transition between two such phases. In many cases, this transition has been linked to a loss of fixed point stability and the emergence of unstable fixed points whose number is exponentially large in the dimension of the system [18–20]. However, unique to the ecological case is the emergence of long timescales in the fluctuating phase and

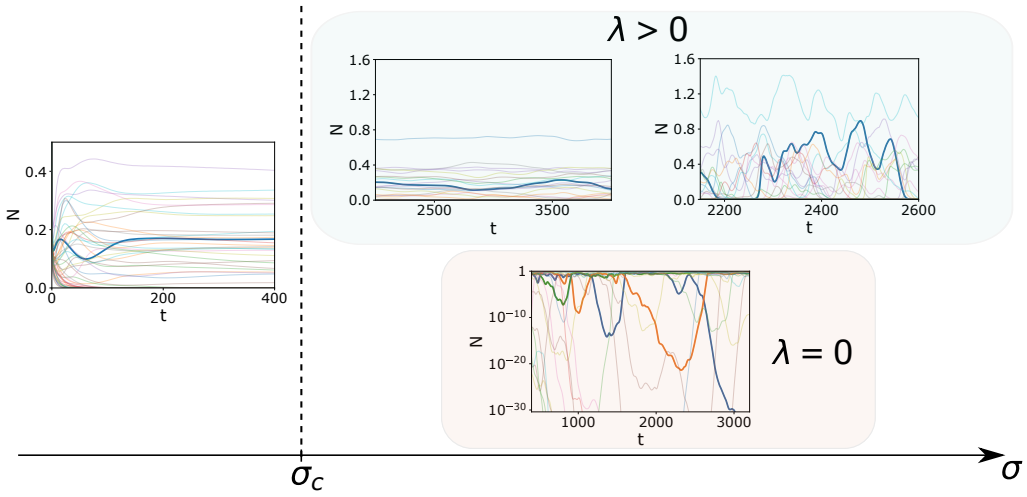

Figure 1: **Phases of the Lotka-Volterra dynamics.** Example degrees of freedom from a simulation of the dynamics Eq. (1) with $\mu = 10$ and $S = 4000$ for increasing values of σ. When $\sigma < \sigma_c$, the dynamics reach a fixed point. When $\lambda > 0$ and $\sigma > \sigma_c$ the dynamics reach a time-translation invariant state. The amplitude of the time-fluctuations grows with σ, and their correlation time decreases with σ. When $\lambda = 0$ and $\sigma > \sigma_c$, the dynamics is aging, with growing fluctuations of log-populations sizes. Shown are simulations with $\delta\sigma = \sigma - \sigma_c = -0.3$ (left); $\lambda = 10^{-8}, \delta\sigma = 0.1$ (upper center); $\lambda = 10^{-8}, \delta\sigma = 0.4$ (upper right); and $\delta\sigma = 0.4$ (lower right).

the associated large fluctuations [11–13]. This is fundamentally due to the time-derivative of population sizes automatically becoming small when population sizes are small, a behavior recently called "stickiness" [1] and leading to possible heteroclinic networks [21]. As we show below, this has striking consequences on the dynamics close to the transition.

In this work, we focus on the canonical Lotka-Volterra dynamics. The dynamics of the population sizes N_i of the species $i = 1 \dots S$, with $S \gg 1$ the number of species, in a well-mixed system (no spatial extension), read [22–24]

$$\dot{N}_i = N_i \left(1 - N_i - \sum_j \alpha_{ij} N_j \right) + \lambda \,. \tag{1}$$

The matrix α_{ij} quantifies the interactions between species, and λ accounts for migration of individuals into the community from its surroundings. In Eq. (1), time has been rescaled by the generation time and population sizes by their long-time value in the absence of interactions. We consider randomly sampled interaction matrices with independent and identically-distributed entries, such that $\text{mean}(\alpha_{ij}) = \mu/S$ and $\text{std}(\alpha_{ij}) = \sigma/\sqrt{S}$. As the parameter σ is increased and crosses a critical value σ_c, the system exhibits a transition between a fixed point phase and a fluctuating one [6, 25], see Fig. 1 for representative trajectories generated by Eq. (1). The biological relevance of such theoretical descriptions was demonstrated experimentally in [26].

As mentioned above, we have recently shown that in the fluctuating phase, the system collectively self-organizes to evolve over long timescales when the migration rate is small but positive [11], $0 < \lambda \ll 1$. In this regime, the abundance of every species exhibits exponential growth and decline between high values of order $O(1)$ and low values of order $O(\lambda)$, inducing a turnover in the identity of the most abundant species over time, see Fig. 2. This is accompanied by the emergence of a long correlation timescale, that scales as $O(|\ln \lambda|)$.

In the absence of migration, when $\lambda = 0$, the above-mentioned timescale diverges and

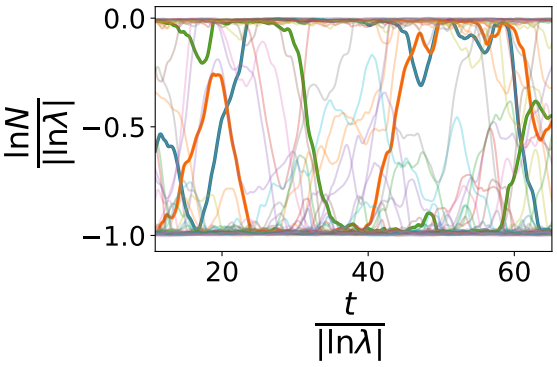

Figure 2: **Slow dynamics in the fluctuating phase with small migration rate ($0 < \lambda \ll 1$).** Example degrees of freedom from a simulation of the dynamics of a community of interacting species following Eq. (1), showing exponential growth and decline of abundances between $O(\lambda)$ and $O(1)$, over timescales of order $|\ln\lambda|$. This is formalized by considering the process $z(s)$ with $s = t/|\ln\lambda|$ and $z = \ln N/|\ln\lambda|$, that converges as $\lambda \to 0^+$ to a time-translation invariant process with finite correlation time, confined between 0 and -1. Here $\lambda = 10^{-40}$, $\mu = 10$, $\sigma - \sigma_c = 0.4$ and $S = 4000$.

instead one finds aging dynamics where the correlation time grows as the age t of the system [11–13]. At the same time, the logarithm of the population sizes of the different species experience ever larger fluctuations between high values of order $O(1)$ and low values of order $O(-t)$, see the $\lambda = 0$ panel of Fig. 1. This aging regime is very different from the one observed in standard glasses with an rough energy landscape–or in the Lotka-Volterra model with migration and symmetric interactions [27, 28]. In fact, the slow dynamics emerging when $\lambda = 0$ and when $\lambda \ll 1$ can be thought of as high-dimensional generalizations of the rock-paper-scissors dynamics [29] (a three-species dynamics where A inhibits the growth of C, C inhibits B and B inhibits A), in which the dynamics ever slows down as the system gets ever closer to the heteroclinic cycle connecting three unstable fixed points (one for each species alone). Crucially, unlike in low dimension where this mechanism requires a specific structure of the interaction matrix, it appears to generically emerge in high-dimensional population dynamics models [11, 13, 21]. However, in this high-dimensional generalization, dynamics do not follow cycles and the system always exhibits a large number of species with high abundances. Taken together, these results highlight the crucial role that migration might play in setting the timescale over which population sizes fluctuate in real ecosystems.

Understanding the behavior of these dynamics in the critical regime close to the transition, and how they are affected by the migration rate λ, has so far remained an open problem. Earlier numerical work [12] showed that, as the transition is approached from $\sigma > \sigma_c$, the amplitude of the fluctuations continuously vanishes, and timescales grow, see the $\lambda > 0$ panels of Fig. 1, but the precise scaling behavior has not been elucidated.

In this work, we provide a comprehensive analytical description of the critical regime of the Lotka-Volterra dynamics Eq. (1) when σ goes to σ_c from above, meaning from inside the fluctuating phase. Our main contribution is to identify three different universality classes, and compute in each of them the two critical exponents relating the growth of fluctuations and the divergence of timescales to the distance to the critical point. We show that these three universality classes depend on the relative size of the migration rate λ and the distance to the transition $\sigma - \sigma_c$, corresponding to the different regions of parameter space sketched in Fig. 3(a). One scaling regime is obtained when $\lambda = 0$, where the transition point $\sigma = \sigma_c$ separates a fixed point phase from an aging phase. Another scaling regime is obtained when the limit

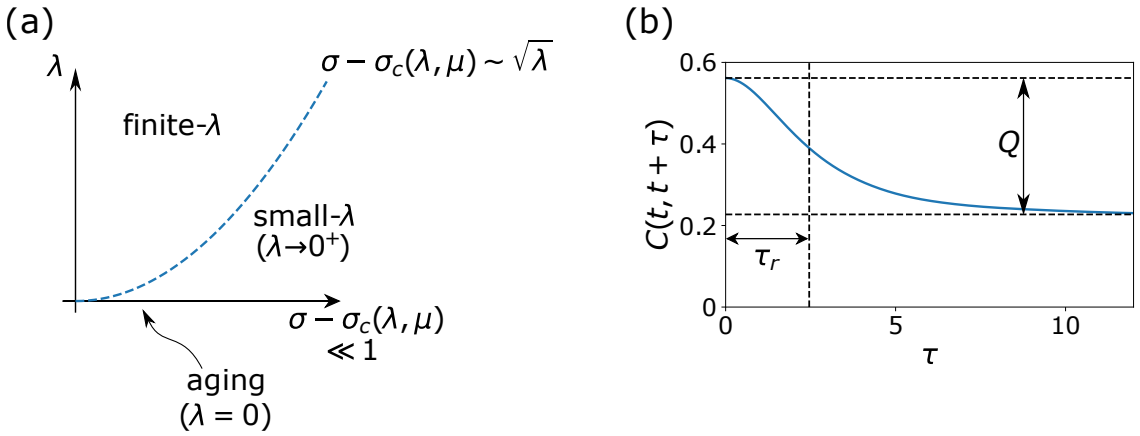

Figure 3: **Critical regimes of the Lotka-Volterra dynamics.** **(a)** Three different scaling regimes are identified when $\sigma - \sigma_c$ is small: when $\lambda = 0$; when $\lambda > 0$ and fixed; and in the limit $\lambda \to 0^+$, taken before the limit $\sigma \to \sigma_c^+$. The crossover between the second and third regimes takes place at $\sigma - \sigma_c \sim \sqrt{\lambda}$. **(b)** Two-time autocorrelation function $C(t,t') \equiv \sum_i N_i(t)N_i(t')/S$ in the fluctuating phase, with definitions of the order parameters Q (the amplitude of the fluctuations) and τ_r (the relaxation time of the fluctuations). As the critical point is approached from above, $\sigma \to \sigma_c^+$, Q decreases and τ_r increases. Here $C(t,t')$ is shown for $\lambda = 0.1$, $\mu = 10$ and $\sigma - \sigma_c = 0.1$.

$\lambda \to 0^+$ is taken before the limit $\sigma - \sigma_c \to 0^+$, in which case the transition point separates a fixed point phase from a phase with time-translation invariant statistics with a diverging timescale. Lastly, a third scaling regime is obtained when $\sigma - \sigma_c \to 0^+$ for $\lambda > 0$ fixed, where the transition is from a fixed point phase to a time-translation invariant chaotic phase with finite correlation time. Only this last transition bears similarity with that observed in models of random neural networks and in fact, as we show, it is characterized by the same set of critical exponents as that of such models with a strongly non-linear transfer function [30]. Additionally, we find the position of the critical point $\sigma_c(\lambda,\mu)$ for arbitrary values of λ and μ, generalizing earlier results [6] showing that $\sigma_c(\lambda = 0,\mu) = \sqrt{2}$. We also demonstrate that the chaotic phase does not exist for large values of λ, where the system directly undergoes a transition from a fixed point phase to one of unbounded growth.

The paper is organized as follows. We first present a summary of our main results in Sec. 2. The rest of the paper is dedicated to the derivation of these results. In Sec. 3, we recall the Dynamical Mean Field Theory (DMFT) equations associated to the Lotka-Volterra dynamics, which form the basis of our analysis. We then discuss the two cases $\lambda = 0$ and $\lambda \to 0^+$ in Sec. 4. Lastly, in Sec. 5, we consider the case where the migration rate $\lambda > 0$ is fixed and positive.

2 Summary of the main results

We quantify the near-critical dynamics by evaluating the amplitude of the population sizes fluctuations and their correlation time. For that, we study the two-point correlation function $C(t,t') \equiv \sum_i N_i(t)N_i(t')/S$, and extract from it the amplitude Q and the associated correlation timescale τ_r, which are graphically depicted in Fig. 3 (b). As explained in Sec. 3, the auto-correlation function fully characterizes the long-time trajectories of the abundances. In this section, we summarize our results for each of the three above-mentioned universality classes.

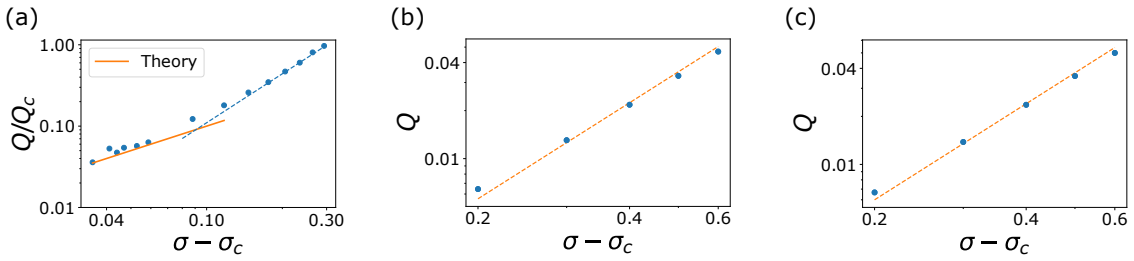

Figure 4: **Growth of fluctuations in the vicinity of the critical point. (a)** $\lambda > 0$ criticality. For small $\sigma - \sigma_c(\lambda, \mu)$ the amplitude of the fluctuations is predicted to grow to leading order as $Q/Q_c = (\sigma - \sigma_c)$ with Q_c a known function of λ and μ. The dots are obtained from numerically solving the DMFT equations of Sec. 3. The solid line is the analytical prediction $Q/Q_c = (\sigma - \sigma_c)$. This is a parameter-free agreement, as Q_c is here known analytically. At larger values of $\sigma - \sigma_c(\lambda, \mu)$ the scaling becomes quadratic, as shown by a fit of the form $Q/Q_c = a\,(\sigma - \sigma_c)^2$ (dashed line). Here $\lambda = 0.1$ and $\mu = 10$. **(b)** $\lambda = 0$ criticality. For small $\sigma - \sigma_c(\lambda = 0, \mu)$, the amplitude of the fluctuations is predicted to grow as $Q \sim (\sigma - \sigma_c)^2$. The dots are obtained from numerically solving the rescaled DMFT equations of Sec. 4.3 and the dashed line is a fit of parameter Q_c to the form $Q = Q_c\,(\sigma - \sigma_c)^2$. Here $\mu = 10$. **(c)** $\lambda \to 0^+$ criticality. For small $\sigma - \sigma_c(\lambda = 0, \mu)$, the amplitude of the fluctuations is predicted to grow as $Q \sim (\sigma - \sigma_c)^2$. The dots are obtained from numerically solving the rescaled DMFT equations of Sec. 4.1 and the dashed line is a fit of parameter Q_c to the functional form $Q = Q_c\,(\sigma - \sigma_c)^2$. Here $\mu = 10$.

2.1 Growth of fluctuations

The average amplitude square Q of the temporal fluctuations of the population sizes is obtained from $C(t, t')$ through

$$Q = \lim_{t \to \infty} \left(C(t, t) - \lim_{\tau \to \infty} C(t, t + \tau) \right). \tag{2}$$

At the transition, there are no fluctuations and $Q = 0$. Entering the fluctuating phase, Q grows continuously with the distance to the critical point $\sigma - \sigma_c$. This growth is characterized by a critical exponent β defined by the scaling relation

$$Q \sim |\sigma - \sigma_c(\lambda, \mu)|^\beta . \tag{3}$$

In the two cases where the limit $\lambda \to 0^+$ is taken before the limit $\sigma \to \sigma_c(0, \mu) = \sqrt{2}$, and when $\lambda = 0$, we obtain the same value $\beta = 2$, see Sec. 4.2 and Sec. 4.4 respectively. A different exponent $\beta = 1$ is found when $\lambda > 0$ fixed. In that case, we managed to obtain a more precise description of the near-critical regime as

$$Q \sim Q_c(\lambda, \mu) |\sigma - \sigma_c(\lambda, \mu)| , \tag{4}$$

where the coefficient $Q_c(\lambda, \mu)$ is a non-universal parameter-dependent amplitude that we determine, see Sec. 5.4. We confirm these predictions in numerical solutions of the DMFT equations established in Sec. 3, see Fig. 4.

2.2 Critical slowing down

We now describe the temporal dynamics of these fluctuations close to the transition, which will provide us with a precise characterization of the timescales involved in the dynamics. At

long times, it is useful to note that the autocorrelation function $C(t,t')$ can be written as a sum of a steady part and a transient part $\delta C(t,t')$,

$$C(t,t') = w^2 + Q\,\delta C(t,t') \tag{5}$$

with $\delta C(t,t) = 1$ and $\lim_{\tau\to\infty} \delta C(t,t+\tau) = 0$. All the information about the time-behavior of the fluctuations is contained in $\delta C(t,t')$.

We start by considering the regime where $\lambda \to 0^+$ before $\sigma - \sqrt{2} \to 0^+$. From Eq. (1), we introduce $g_i(t) \equiv 1 - \sum \alpha_{ij} N_j(t)$ the growth rate of species i at time t. Despite the fact that interaction coefficients are independent and identically distributed, the time-averaged value of g_i is different from species to species, and is in fact Gaussian distributed, see Sec. 3. This is crucial to the behavior of the dynamics near the critical point. The form of the empirical correlation function in Eq. (5) might indeed suggest that all species experience small fluctuations in their population sizes, with typical amplitude $\sqrt{Q}$. This picture is however incomplete and too simplistic. In fact, it is correct only for the most abundant species, whose time-averaged growth rate is of order $O(1)$ and whose population size slightly fluctuates around a finite $O(1)$ time-averaged value. Another group of species are the rarest ones, those whose time-averaged growth rate is negative and of order $O(1)$, that are only rescued by the migration and have very small population sizes of order $O(\lambda)$. As $\lambda \to 0^+$, these do not contribute to the empirical correlation function. In between, there is a small fraction of species, of order $O(\sqrt{Q})$, whose time-averaged growth rate is small and also of order $O(\sqrt{Q})$. These experience large fluctuations in the logarithm of their abundance, that alternates between small values of order $O(\sqrt{Q})$ and much smaller values $O(\lambda)$, as $\lambda \ll \sqrt{Q}$ in this regime. Transition between these two values happen on timescales of order $O(Q^{-1/2}|\ln\lambda|)$, since the growth rate of these species is itself of order $O(\sqrt{Q})$. This argument, together with the dependence of Q near the critical point described above, sets the behavior of the correlation time of $\delta C(t,t')$.

Indeed, in this regime, we find that the naturally slow dynamics in the fluctuating phase, with timescales of order $O(|\ln\lambda|)$ at fixed $\sigma > \sqrt{2}$, is further slowed down in the vicinity of the critical point with a correlation time $\tau_r \sim (\sigma - \sqrt{2})^{-1}|\ln\lambda|$. This leads to the scaling form

$$\delta C(t,t') \sim \delta\hat{C}_+\left(\frac{|t-t'|/|\ln\lambda|}{|\sigma-\sqrt{2}|^{-\zeta}}\right), \tag{6}$$

with $\zeta = 1$ and $\delta\hat{C}_+$ a scaling function, see Sec. 4.2.

We now discuss the case $\lambda = 0$. For $\sigma > \sqrt{2}$ fixed, the dynamics is aging with a correlation time that grows linearly with the elapsed time t, meaning that the long-time correlation function becomes time-translation invariant in log-time. Close to the transition, we also find that only a small fraction $O(\sqrt{Q})$ of the species, those with time-averaged growth rate of order $O(\sqrt{Q})$, experience large fluctuations in the logarithm of their population sizes. However, we find that there is no extra slowing down of the aging dynamics in the vicinity of the critical point. In fact, after some long time t, the log-population size of these species fluctuates between small values of order $O(\ln(Q))$ and much smaller values $O(-t\sqrt{Q})$. These transitions happen on timescales of order $O(t)$, which does not scale with Q, since growth rates are of order $O(\sqrt{Q})$ for those species. In other words, close to the transition, we obtain

$$\delta C(t,t') \sim \delta\hat{C}_0\left(\frac{|\ln t - \ln t'|}{|\sigma-\sqrt{2}|^{-\zeta}}\right), \tag{7}$$

with $\zeta = 0$ and $\delta\hat{C}_0$ a scaling function, see Sec. 4.4.

When $\lambda > 0$ fixed, the dynamics in the fluctuating phase reach a time-translation invariant state with a finite correlation time, that is $\delta C(t,t') \to \delta C(t-t')$ at long times. At odds with the previously discussed results, close to the transition, all species experience small fluctuations of

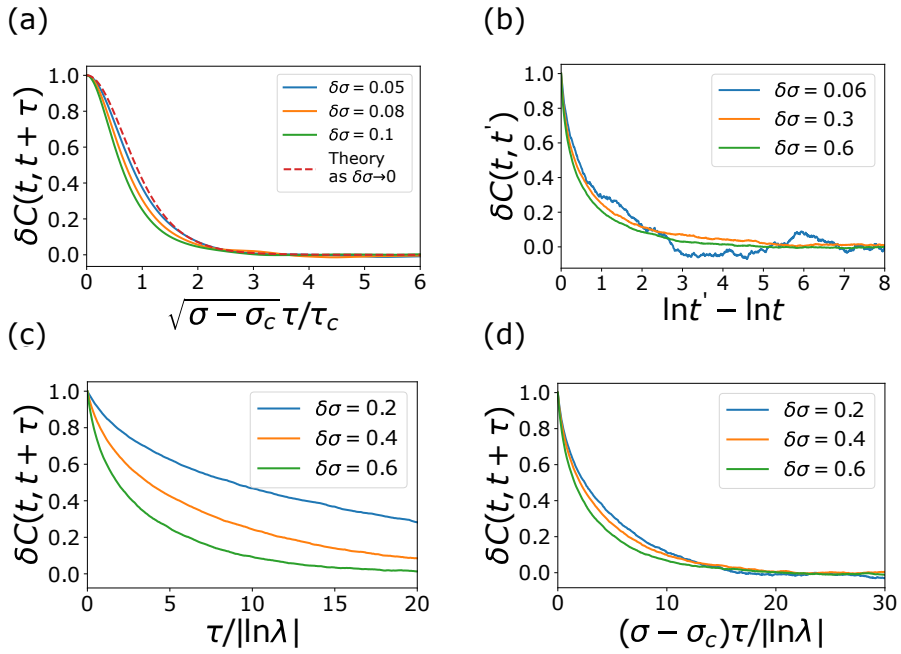

Figure 5: **Growth of timescales in the vicinity of the critical point. (a)** $\lambda > 0$ criticality. For small $\delta\sigma = \sigma - \sigma_c(\lambda,\mu)$, the rescaled correlation function $\delta C(t, t+\tau)$ converges to the scaling form given in Eq. (8). The continuous lines are obtained by numerically solving the DMFT equation of Sec. 3. This is a parameter-free agreement: the dashed red line is the analytical prediction of Eq. (8), and $\tau_c(\lambda,\mu)$ is known. Here $\lambda = 0.1$ and $\mu = 10$. **(b)** $\lambda = 0$ criticality. For small $\delta\sigma = \sigma - \sqrt{2}$, the rescaled correlation function converges to the scaling form of Eq. (7). Note the collapse of the correlation functions for different values of $\delta\sigma$ without rescaling of the log-time axis. The continuous lines are obtained by numerically solving the DMFT equation of Sec. 4.3. Here $\mu = 10$. **(c, d)** $\lambda \to 0^+$ criticality. **(c)** The correlation time of the fluctuations diverge as $\sigma \to \sqrt{2}$ from above. **(d)** For small $\delta\sigma = \sigma - \sqrt{2}$, the timescale in rescaled time grows as $(\sigma - \sqrt{2})^{-1}$. The continuous lines are obtained by numerically solving the DMFT equation of Sec. 4.1. Here $\mu = 10$.

order $O(\sqrt{Q})$ of their population size around a value set by their time-averaged growth rate. At the critical point, it is known that the fixed point reached by the dynamics is marginally stable [31]. Beyond the critical point, unstable directions are thus nearly marginal, giving rise to slow fluctuations. We obtain the entire correlation function close to the transition, see Sec. 5.3, which reads

$$\delta C(t,t') \sim 1 - \mathrm{Tanh}^2\left(\frac{|t-t'|}{\tau_c(\lambda,\mu)|\sigma-\sigma_c(\lambda,\mu)|^{-\zeta}}\right), \tag{8}$$

with the critical exponent $\zeta = 1/2$ and $\tau_c(\lambda,\mu)$ a non-universal timescale that we characterize in Sec. 5.4. We confirm these predictions in numerical solutions of the Dynamical Mean Field Theory equations established in Sec. 3, see Fig. 5.

2.3 Crossover between the finite $\lambda > 0$ and the $\lambda \to 0^+$ critical behaviors

In this section, we discuss the crossover existing between the two universality classes defined by $\lambda > 0$ and $\lambda \to 0^+$. We start by describing the dynamics obtained when the limit $\lambda \to 0^+$ is taken after the limit $\sigma \to \sigma_c(\lambda,\mu)$. We show in Sec. 5.6 that a small amount of migration stabilizes the fixed point phase and that the shift in the position of the critical point is propor-

tional to $\sqrt{\lambda}$, meaning $\sigma_c(\lambda,\mu)-\sqrt{2}\sim\sqrt{\lambda}$ at small λ. We also show that the amplitude of the critical fluctuations $Q_c(\lambda,\mu)$, see Eq. (4), becomes vanishingly small in this regime and we get

$$Q\sim\sqrt{\lambda}\,|\sigma-\sigma_c(\lambda,\mu)|\,,$$

see Eq. (57) in Sec. 5.6. At the same time, the timescale $\tau_c(\lambda,\mu)$ in Eq. (8) increases with decreasing λ and we get the timescale

$$\tau_c(\lambda,\mu)|\sigma-\sigma_c(\lambda,\mu)|^{-1/2}\sim\lambda^{-1/4}\,|\sigma-\sigma_c(\lambda,\mu)|^{-1/2}\,,$$

see Eq. (58) in Sec. 5.6. On the other hand, when the limit $\lambda\to 0^+$ is taken before the limit $\sigma\to\sqrt{2}$, we obtain Eq. (6) and Eq. (3) with $\beta=1$, showing that the correlation time and the amplitude of the fluctuations behave as $|\sigma-\sqrt{2}|^{-1}$ and $|\sigma-\sqrt{2}|^2$ respectively. Therefore, when both $\lambda\ll 1$ and $\sigma-\sqrt{2}\ll 1$, one observes a crossover between these two regimes at $\sigma-\sqrt{2}\sim\sqrt{\lambda}$. The finite $\lambda>0$ critical regime dominates for $\sigma-\sqrt{2}\ll\sqrt{\lambda}$ while the $\lambda\to 0^+$ critical regime dominates when $\sigma-\sqrt{2}\gg\sqrt{\lambda}$. The crossover is illustrated in Fig. 4 (a).

3 Dynamical mean-field theory

Our theory is built on dynamical mean-field theory (DMFT). Originally developed in the context of spin-glasses [32], and later adapted to ecological dynamics in [5] and to the present equations in [12,25], it shows that in the limit $S\to\infty$ and for N_i sampled independently at the initial time, the dynamics of the population sizes are described by independent realizations of the stochastic differential equation

$$\dot{N}(t)=N(t)[1-N(t)-\mu m(t)+\sigma\xi(t)]+\lambda\,, \tag{9}$$

where the index i has been dropped, and where $\xi(t)$ is a zero-mean Gaussian process and $m(t)$ a deterministic function of time. This can be shown to come from the fact that the term $\xi_i(t)\equiv\sum_j\alpha_{ij}N_j(t)$ in Eq. (1) is the sum of many weakly-correlated contributions. However, $m(t)$ and the correlations of $\xi(t)$ are not provided in advance. Instead, they are derived through self-consistency conditions. This is a dynamical equivalent of the self-consistency condition on the magnetization derived in the mean-field Ising model, for instance. Recalling that $\langle\alpha_{ij}\rangle=\mu/S$ and $\langle\alpha_{ij}\alpha_{kl}\rangle-\langle\alpha_{ij}\rangle\langle\alpha_{kl}\rangle=\sigma^2\delta_{ik}\delta_{kl}/S$, the self-consistency conditions read

$$m(t)=\langle N(t)\rangle\,, \tag{10}$$

and

$$\left\langle\xi(t)\xi(t')\right\rangle=\left\langle N(t)N(t')\right\rangle\,, \tag{11}$$

where the average $\langle\ldots\rangle$ stands for an average over the stochastic process in (9). Because $\xi(t)$ is a Gaussian process, obtaining the first two moments of the population size $\langle N(t)\rangle$ and $\left\langle N(t)N(t')\right\rangle$ allows to completely characterize the dynamics of $N(t)$ by using Eq. (9).
We denote by m_∞ the steady-state value of $m(t)$. At long-times, we further decompose the noise $\xi(t)$ into a frozen Gaussian random variable $\bar{\xi}$ and a Gaussian process $\delta\xi(t)$ that completely decorrelates over time, meaning $\xi(t)\equiv\bar{\xi}+\epsilon\delta\xi(t)$ with $\lim_{\tau\to\infty}\langle\delta\xi(t)\delta\xi(t+\tau)\rangle=0$. The amplitude ϵ of the fluctuating part is defined so that $\left\langle\delta\xi(t)^2\right\rangle=1$. Using the self-consistency condition Eq. (11), we get from the decomposition in Eq. (5) that $\left\langle\bar{\xi}^2\right\rangle=w^2$ and $\langle\delta\xi(t)\delta\xi(t+\tau)\rangle=\delta C(t,t+\tau)$ together with $Q=\epsilon^2$. To make the notations more compact, especially in Sec. 4, we introduce the time-averaged growth rate $g\equiv(1-\mu m_\infty)+\sigma\bar{\xi}$ and $\tilde{m}\equiv 1-\mu m_\infty$. The dynamics in Eq. (9) then becomes at long-times

$$\dot{N}(t)=N(t)[g+\epsilon\sigma\delta\xi(t)-N(t)]+\lambda\,. \tag{12}$$

The random variable g is Gaussian distributed with yet unknown mean and variance. Its distribution is denoted $P(g)$ and is given by

$$P(g) = \frac{1}{\sqrt{2\pi} w\sigma} \exp\left(-\frac{(g-\tilde{m})^2}{2w^2\sigma^2}\right). \tag{13}$$

It is finally interesting to note that $N(t)$ defined in Eq. (9) is a non-Gaussian process, so that the methods used to solve the DMFT equations for random recurrent neural networks [15,30,33] do not apply.

4 Critical regimes when $\lambda \to 0^+$ and $\lambda = 0$

In this section, we determine the properties of the dynamical phase transition first when the limit $\lambda \to 0^+$ is taken before the limit $\sigma \to \sqrt{2}$, and then when $\lambda = 0$. As discussed in Sec. 2.3, the former regime is relevant when $\lambda \ll \sigma - \sqrt{2} \ll 1$.

In those two cases, for any $\sigma > \sqrt{2}$ finite, it was shown in [11], that the dynamics evolve over long timescales. When $\lambda \to 0^+$, the dynamics reach a steady-state that is time-translation invariant with a long correlation time proportional to $|\ln\lambda|$, meaning that

$$\lim_{\lambda\to 0^+} \delta C_\lambda(t, t + |\ln\lambda| s) \to \delta\hat{C}_+(s), \tag{14}$$

with $\delta\hat{C}_+(s)$ a regular function as $s \to 0^+$. On the other hand, in the absence of migration ($\lambda = 0$), the dynamics do not reach a steady-state, but instead are time-translation invariant in log-time

$$\lim_{t\to\infty} \delta C_{\lambda=0}(t, te^s) = \delta\hat{C}_0(s),$$

with $\delta\hat{C}_0(s)$ another regular function as $s \to 0^+$. This is typical of aging dynamics, with a growth of timescale proportional to the age of the system. Leveraging these two relations, effective equations for the long-time dynamics of the population size $N(t)$ were obtained in [11]. Below, these long-time effective dynamics are reviewed in Sec. 4.1 and Sec. 4.3, for dynamics with $\lambda \to 0^+$ and $\lambda = 0$ respectively. In Sec. 4.2 and Sec. 4.4, we use these effective dynamics as a starting point to infer the properties of the near-critical regime.

4.1 Steady-state dynamics when $\lambda \to 0^+$

When $\lambda \to 0^+$ and $\sigma - \sqrt{2} > 0$ fixed, the effective steady-state dynamics is described by a rescaling of the original DMFT equations Eq. (12).. Following [11], we briefly recall the transformations allowing to describe this long-time dynamics. First, we introduce $z = \ln N/|\ln\lambda|$ and $s = t/|\ln\lambda|$. From Eq. (12), we get

$$z'(s) = g + \sigma\epsilon\delta\hat{\xi}(s) - W_\lambda(z) + W_\lambda(-z-1),$$

where $W_\lambda(z) = \exp(|\ln\lambda| z)$. Here $\delta\hat{\xi}(s) \equiv \delta\xi(t)$ is a zero-mean Gaussian noise with well-defined correlations $\delta\hat{C}_+(s)$ when $\lambda \to 0^+$, as follows from Eq. (14). Note that when $z > 0$, $W_\lambda(z) \to +\infty$ when $\lambda \to 0^+$, while $W_\lambda(z) \to 0$ for $z < 0$. Therefore, in the limit $\lambda \to 0^+$, the process $z(s)$ follows a well-defined stochastic differential equation [11],

$$z'(s) = g + \sigma\epsilon\delta\hat{\xi}(s) - W(z) + W(-z-1) \tag{15}$$

where $W(z)$ acts as a hard wall with $W(z > 0) = +\infty$ and $W(z < 0) = 0$, so that the dynamics are confined in $-1 \le z \le 0$. The DMFT equations in (10, 11) however require to express $N(s)$

in terms of the noise $\delta\hat{\xi}(s)$. Note that for any λ, $N(s) = W_\lambda(z(s))$. Additionally, when $\lambda \to 0^+$, the confining force exerted by the effective hard-wall must exactly compensate the drive on the dynamics of $z(s)$ when $z(s) = 0$. Therefore, Eq. (15) is supplemented by an expression for $N(s)$ valid at long times,

$$N(s) = \Theta(z(s))\left(g + \sigma\epsilon\delta\hat{\xi}(s)\right), \tag{16}$$

where the Heaviside function Θ is used with the convention $\Theta(0) = 1$. Therefore, the system of self-consistency equations in the $\lambda \to 0^+$ regime reads

$$\frac{1-\tilde{m}}{\mu} = \left\langle \Theta(z(s))\left(g + \epsilon\sigma\delta\hat{\xi}(s)\right)\right\rangle, \tag{17}$$

and

$$w^2 + \epsilon^2\delta\hat{C}_+(s) = \left\langle \Theta(z(s))\Theta(z(0))\left(g + \epsilon\sigma\delta\hat{\xi}(s)\right)\left(g + \epsilon\sigma\delta\hat{\xi}(0)\right)\right\rangle, \tag{18}$$

where all averages are performed in the steady state. The dynamics of the many-body dynamics in Eq. (1) at small λ, showing the effective confined stochastic process Eq. (15) are shown in Fig. 2.

4.2 Growth of fluctuations and timescales when $\lambda \to 0^+$

Equation (18), together with the dynamics in Eq. (15), gives us the self-consistency equation satisfied by the correlation function $\delta\hat{C}_+(s)$. When $\epsilon \ll 1$, we claim that fluctuations are primarily generated by the small fraction of populations whose time-averaged growth rate g is of order $O(\epsilon)$. Indeed, if $g > 0$ and of order $O(1)$, Eq. (15) implies that exponentially rare large fluctuations of the noise $\delta\hat{\xi}$ are needed to get $z(s) < 0$, while for $g < 0$ and of order $O(1)$, it implies that $z(s) > 0$ is also an exponentially rare event in ϵ. Considering only contributions where $g \sim O(1)$ and neglecting exponentially small terms thus amounts to replacing $\Theta(z(s))$ by $\Theta(g)$, and the self-consistency equation would become

$$w^2 + \epsilon^2\delta\hat{C}_+(s) = \left(\left\langle\Theta(g)g^2\right\rangle + \epsilon^2\sigma^2\delta\hat{C}_+(s)\right), \tag{19}$$

from which no solution for $\delta\hat{C}_+(s)$ respecting $\delta\hat{C}_+(0) = 1$ and $\delta\hat{C}_+(\infty) = 0$ can be obtained. This motivates the need to properly take into account the effect of populations with small time-averaged growth rate $g \sim O(\epsilon)$. The critical exponents β and ζ introduced in Sec. 2 are then obtained by requiring that the amplitude of these contributions is such that there exists a well-behaved solution of the DMFT equations. More precisely, when the temporal fluctuations $\epsilon\delta\hat{\xi}(s)$ are small, only species whose time-averaged growth rate g is $O(\epsilon)$ show any significant fluctuations in their $\ln N$ values. The instantaneous growth rates of those that do is of order ϵ (negative or positive), and so the exponential growth and decline of N between $O(\lambda)$ and $O(1)$ (see Fig. 2) takes a time of order $|\ln\lambda|/\epsilon$. As, by definition, $Q \sim \epsilon^2$ this explains the scaling relation $\beta = \zeta/2$. We now formalize these results, also allowing us to obtain the scaling of ϵ with the distance from the critical point.

To proceed, in the right-hand side of Eq. (18), we split the average over g between (i) $g > 0$, in which case $\Theta(z) = 1$ with high probability for small ϵ, and (ii) $g < 0$ in which case $\Theta(z) = 0$ with high probability for small ϵ. We can obtain from Eq. (18),

$$\begin{aligned} w^2 + \epsilon^2\delta\hat{C}_+(s) = &\int_0^{+\infty} \mathrm{d}g\, P(g)\left(g^2 + \epsilon^2\sigma^2\delta C_+(s)\right) \\ &+ \int_{-\infty}^{+\infty} \mathrm{d}g\, P(g)\left\langle[\Theta(z(s))\Theta(z(0)) - \Theta(g)]\left(g + \epsilon\,\sigma\delta\hat{\xi}(0)\right)\left(g + \epsilon\,\sigma\delta\hat{\xi}(s)\right)\right\rangle_g \end{aligned} \tag{20}$$

where $\langle \dots \rangle_g$ denotes an average over realizations of the noise $\delta\hat{\xi}$ at fixed g. As argued above, the only perturbative contributions to the second integral arise from values $g = O(\epsilon)$. We therefore introduce $\tilde{g} \equiv g/\epsilon$, rescale time as $\tilde{s} = \epsilon s$, and denote $\tilde{z}(\tilde{s}) \equiv z(\tilde{s}/\epsilon)$. $\tilde{z}(\tilde{s})$ satisfies an equation like that of the original process $z(s)$ in Eq. (15), but with an $O(1)$ fluctuating noise,

$$\frac{\mathrm{d}\tilde{z}}{\mathrm{d}\tilde{s}} = \tilde{g} + \sigma\delta\xi(\tilde{s}) - W(\tilde{z}) + W(-\tilde{z}-1). \tag{21}$$

In terms of this process, and after performing the first integral in the right-hand side of Eq. (20), we get

$$\left(1-\frac{\sigma^2}{2}\right)\left(w^2+\epsilon^2\delta\hat{C}_+(\tilde{s})\right)+\frac{\sigma^2}{2}\left(w^2+\epsilon^2\delta\hat{C}_+(\tilde{s})\right)\mathrm{Erf}\left(\frac{\tilde{m}}{\sqrt{2}w\sigma}\right) + \frac{\tilde{m}^2}{2}\left[1+\mathrm{Erf}\left(\frac{\tilde{m}}{\sqrt{2}w\sigma}\right)\right]+\frac{\tilde{m}w}{\sqrt{2\pi}\sigma}\exp\left(-\frac{\tilde{m}^2}{2w^2\sigma^2}\right) = \epsilon^3 I(\tilde{s}). \tag{22}$$

where we have introduced

$$I(\tilde{s}) = \int_{-\infty}^{+\infty} \mathrm{d}\tilde{g}\, P(\epsilon\tilde{g})\left\langle [\Theta(\tilde{z}(\tilde{s}))\Theta(\tilde{z}(0)) - \Theta(\tilde{g})](\tilde{g}+\sigma\delta\xi(0))(\tilde{g}+\sigma\delta\xi(\tilde{s}))\right\rangle_{\tilde{g}}.$$

Assuming that the statistics of $\delta\xi(\tilde{s})$ are independent of ϵ, meaning that the typical timescale over which fluctuations of $\delta\xi(s)$ take place behaves as ϵ^{-1}, we obtain that $I(\tilde{s})$ has a finite limit $I_0(\tilde{s})$ when $\epsilon \to 0$ and $\sigma \to \sqrt{2}$ given by

$$I_0(\tilde{s}) = P(0)\int_{-\infty}^{+\infty} \mathrm{d}\tilde{g}\left\langle [\Theta(\tilde{z}(\tilde{s}))\Theta(\tilde{z}(0)) - \Theta(\tilde{g})]\left(\tilde{g}+\sqrt{2}\delta\xi(0)\right)\left(\tilde{g}+\sqrt{2}\delta\xi(\tilde{s})\right)\right\rangle_{\tilde{g}}. \tag{23}$$

In fact, when $|\tilde{g}|$ is large, $\Theta(\tilde{z}(\tilde{s}))\Theta(\tilde{z}(0)) - \Theta(\tilde{g}) = 0$ with large probability, which guarantees the convergence of the above integral. Using the conditions $\delta\hat{C}_+(0) = 1$ and $\delta\hat{C}_+(\infty) = 0$, we get from Eq. (22) the leading order equation satisfied by the correlation function

$$\delta\hat{C}_+(\tilde{s}) = \frac{I_0(\tilde{s}) - I_0(\infty)}{I_0(0) - I_0(\infty)}. \tag{24}$$

This equation cannot be solved explicitly since the average entering Eq. (23) cannot be performed. However, both Eq. (24) and the dynamical equation (21), after setting $\sigma \to \sqrt{2}$, are parameter-free and thus allow to formally determine $\delta\hat{C}_+(\tilde{s})$ to lowest order near the critical point. Given $\delta\hat{C}_+(\tilde{s})$, we are then left with three equations to solve for $\tilde{m}$, w and ϵ near the transition, allowing us to find how the amplitude ϵ scales with the distance from the critical point $\delta\sigma$. Two such equations are obtained by considering Eq. (22) with $\tilde{s} = \infty$ and $\tilde{s} = 0$, yielding to leading order

$$\left(1-\frac{\sigma^2}{2}\right)w^2+\frac{\sigma^2}{2}w^2\mathrm{Erf}\left(\frac{\tilde{m}}{\sqrt{2}w\sigma}\right)+\frac{\tilde{m}^2}{2}\left[1+\mathrm{Erf}\left(\frac{\tilde{m}}{\sqrt{2}w\sigma}\right)\right]+\frac{\tilde{m}w}{\sqrt{2\pi}\sigma}\exp\left(-\frac{\tilde{m}^2}{2w^2\sigma^2}\right) = \epsilon^3 I_0(\infty). \tag{25}$$

and

$$\epsilon^{-1}\left(1-\frac{\sigma^2}{2}+\frac{\sigma^2}{2}\mathrm{Erf}\left(\frac{\tilde{m}}{\sqrt{2}w\sigma}\right)\right) = I_0(0) - I_0(\infty). \tag{26}$$

The third one is obtained by applying a similar reasoning to the first moment equation (17), which yields to leading order,

$$\left(\frac{1}{\mu}-\frac{\sigma w}{\sqrt{2\pi}}\right)-\frac{\tilde{m}}{\mu}-\frac{\sigma w}{\sqrt{2\pi}}\left[\exp\left(-\frac{\tilde{m}^2}{2w^2\sigma^2}\right)-1\right]-\frac{\tilde{m}}{2}\left[1+\mathrm{Erf}\left(\frac{\tilde{m}}{\sqrt{2}w\sigma}\right)\right] = \epsilon^2 J, \tag{27}$$

with

$$J = P(0)\int_{-\infty}^{+\infty} \mathrm{d}\tilde{g}\,\left\langle [\Theta(\tilde{z}(\tilde{s}))-\Theta(\tilde{g})]\left(\tilde{g}+\sqrt{2}\delta\xi(\tilde{s})\right)\right\rangle_{\tilde{g}}\,.$$

At the transition, $\sigma = \sqrt{2}$, $\tilde{m} = 0$, $w = \sqrt{\pi}/\mu$ and $\epsilon = 0$. Close to the transition, for $\sigma = \sqrt{2}+\delta\sigma$ with $0 < \delta\sigma \ll 1$, we expand

$$\tilde{m} = m_1\delta\sigma + m_2\delta\sigma^2 + \dots\,,$$

and

$$w = \frac{\sqrt{\pi}}{\mu}\left(1 + w_1\delta\sigma + \dots\right),$$

and lastly

$$\epsilon = \epsilon_1\delta\sigma + \dots \tag{28}$$

The form of the expansion for the amplitude ϵ of the fluctuations in Eq. (28) is imposed by Eq. (26), recalling that $\sigma = \sqrt{2}+\delta\sigma$. It turns out that the first corrections to $\tilde{m}$ and w can be derived explicitly from Eqs. (25, 27) alone. We find that $\tilde{m}$ agrees with the analytical continuation of the fixed point branch [6] up to order $O\left(\delta\sigma^2\right)$ with

$$m_1 = -\frac{\pi}{\sqrt{2}\mu} \quad \text{and} \quad \mathrm{m}_2 = \frac{-4\pi^2+2\pi\mu-3\pi^2\mu}{16\mu^2}\,, \tag{29}$$

while w agrees with the analytical continuation of the fixed point branch up to order $O(\delta\sigma)$ with

$$w_1 = \frac{2\pi-2\mu+\pi\mu}{2\sqrt{2}\mu}\,. \tag{30}$$

To lowest order, Eq. (26) gives the expression of the amplitude of fluctuations close to the critical point

$$\epsilon_1 = \frac{\pi}{2\mu\left(I_0(\infty)-I_0(0)\right)}\,. \tag{31}$$

Since $Q = \epsilon^2$, and $\epsilon \simeq \epsilon_1\delta\sigma$ with ϵ_1 finite, we obtain the value of the critical exponent

$$\beta = 2\,,$$

as defined through Eq. (4). The expression for ϵ_1 is not explicit, as it relies of the solution of the nonlinear equation Eq. (24) for the correlation function, so the non-universal amplitude Q_c appearing in Eq. (4) is not known explicitly. However, since $I_0(\infty)$ and $I_0(0)$ are both independent of μ, we can conclude that the amplitude of the fluctuations in the near-critical region decreases with the average interaction strength. Additionally, the rescaling of time used to obtain Eq. (24) entails the scaling exponent

$$\zeta = \beta/2 = 1\,.$$

4.3 Steady-state dynamics when $\lambda = 0$

When $\lambda = 0$, the long-time dynamics can be described in a similar way using a Lamperti transformation of the original equations of motion Eq. (12), see Fig. 6. We introduce $z = \ln N/t$ and $s = \ln t$. When $t \to \infty$, the process $z(s)$ follows a well-defined stochastic differential equation [11],

$$z'(s) = -z(s) + g + \sigma\epsilon\delta\hat{\xi}(s) + W(z)\,, \tag{32}$$

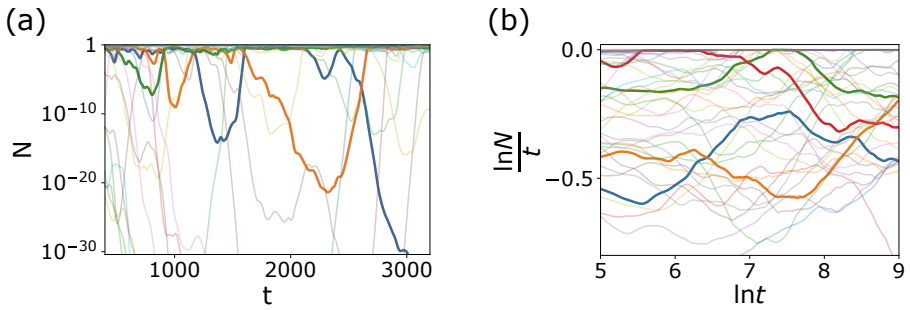

Figure 6: **Aging dynamics at $\lambda = 0$, and time-translation invariant dynamics of the process $z(s)$.** Example degrees of freedom from a simulation of the dynamics Eq. (1). **(a)** Growth of the relaxation time and amplitude of the fluctuations of log-population sizes with the elapsed time in the aging regime. **(b)** Corresponding time-translation invariant process $z(s)$ where $s = \ln t$ and $z = \ln N/t$. Here $\lambda = 0$, $\mu = 10$, $\sigma - \sigma_c = 0.4$ and $S = 4000$.

confined to $z \leq 0$ and with with $\delta\hat{\xi}(s) \equiv \delta\xi(t)$ a zero-mean Gaussian noise with correlations $\delta\hat{C}_0(s)$. The expression for the population size when $\lambda = 0$ remains the same as in Sec. 4.1, with

$$N(s) = \Theta(z(s))\left(g + \epsilon\sigma\delta\hat{\xi}(s)\right).$$

Therefore, the self-consistency conditions Eqs. (17, 18) also hold upon replacing $\delta\hat{C}_+(s)$ by $\delta\hat{C}_0(s)$. The long-time effective dynamics for $\lambda = 0$ and $\lambda \to 0^+$differ by the nature of the process $z(s)$: when $\lambda = 0$, the process is confined on the negative-z side by a harmonic potential, whereas it is confined by another hard wall at $z = -1$ when $\lambda \to 0^+$. This seemingly innocuous difference entails a profound distinction when it comes to critical slowing down. However, the formal resemblance between the two dynamics allows us to investigate their critical property in a similar way.

4.4 Growth of fluctuations when $\lambda = 0$

The calculation for $\lambda = 0$ proceeds similarly to the $\lambda \to 0^+$ case, yet with a crucial difference. When $\lambda \to 0^+$, we obtained to leading order an ϵ-independent equation for the correlation function by introducing the rescaled process $\tilde{z}(\tilde{s}) \equiv z(\tilde{s}/\epsilon)$. Here, one achieves a similar conclusion by rescaling z following $\tilde{z}(s) \equiv z(s)/\epsilon$. From Eq. (32), we find that the latter obeys

$$\frac{\mathrm{d}\tilde{z}}{\mathrm{d}s} = -z + \tilde{g} + \sigma\delta\xi(s) - W(\tilde{z}).$$

The rest follows as before and to leading order,

$$\delta\hat{C}_0(s) = \frac{I_0(\infty) - I_0(s)}{I_0(\infty) - I_0(0)}, \tag{33}$$

with

$$I_0(s) = P(0)\int_{-\infty}^{+\infty} \mathrm{d}\tilde{g}\, \langle[\Theta(\tilde{z}(s))\Theta(\tilde{z}(0)) - \Theta(\tilde{g})](\tilde{g} + \sigma\delta\xi(0))(\tilde{g} + \sigma\delta\xi(s))\rangle_{\tilde{g}}\,.$$

The expansion around $\sigma = \sqrt{2}$ of $\tilde{m}$, w and ϵ remains the same. Thus Eqs. (29, 30, 31) remain valid and the exponent

$$\beta = 2$$

is preserved. The absence of rescaling of time to obtain Eq. (33) entails the scaling exponent

$$\zeta = 0 \,,$$

showing that there is no extra slowing down of the aging dynamics when approaching the transition.

5 Finite λ criticality

In this section, we now interest ourselves to the critical regime obtained when $\sigma - \sigma_c(\lambda,\mu) \to 0^+$ at fixed $\lambda > 0$. Note that here the critical value σ_c must be determined, since it is affected by λ. At the critical point, we denote the mean and variance of the population sizes by $m_\infty = m_c$ and $w = w_c$ respectively. To proceed, it is also convenient to introduce the function

$$\bar{N}(x) = \frac{1 - x + \sqrt{1 - x + 4\lambda}}{2}$$

so that $\bar{N}\left(\mu m_\infty - \sigma\bar{\xi}\right)$ is the long-time solution of Eq. (9) when $\epsilon = 0$. As $\delta\sigma \to 0$ and $\epsilon \to 0$, it is reasonable to expand the equations of motion Eq. (9) around $\bar{N}\left(\mu m_\infty - \sigma\bar{\xi}\right)$ and introduce $\epsilon\delta N \equiv N(t) - \bar{N}\left(\mu m_\infty - \sigma\bar{\xi}\right)$. In terms of these quantities, the self-consistency Eq. (11) becomes

$$\left\langle \bar{N}\left(\mu m_\infty - \sigma\bar{\xi}\right)^2 \right\rangle + 2\epsilon \left\langle \bar{N}\left(\mu m_\infty - \sigma\bar{\xi}\right)\delta N \right\rangle + \epsilon^2 \left\langle \delta N(t)\delta N(t+\tau)\right\rangle = w^2 + \epsilon^2 \left\langle \delta\xi(t)\delta\xi(t+\tau)\right\rangle .$$

Since $\langle \delta\xi(t)\delta\xi(t+\tau)\rangle \to 0$ as $\tau \to \infty$, we can take advantage of the $\tau \to \infty$ limit of the previous equation to obtain

$$\left\langle \bar{N}\left(\mu m_\infty - \sigma\bar{\xi}\right)^2 \right\rangle + 2\epsilon \left\langle \bar{N}\left(\mu m_\infty - \sigma\bar{\xi}\right)\delta N \right\rangle + \epsilon^2 \lim_{\tau\to\infty} \left\langle \delta N(t)\delta N(t+\tau)\right\rangle = w^2 \,, \tag{34}$$

and

$$\left\langle \delta N(t)\delta N(t+\tau)\right\rangle - \lim_{\tau\to\infty} \left\langle \delta N(t)\delta N(t+\tau)\right\rangle = \left\langle \delta\xi(t)\delta\xi(t+\tau)\right\rangle . \tag{35}$$

We also have from Eq. (10)

$$m_\infty = \left\langle \bar{N}\left(\mu m_\infty - \sigma\bar{\xi}\right)\right\rangle + \epsilon \left\langle \delta N\right\rangle . \tag{36}$$

We now proceed by expanding these equations for $\delta\sigma \ll 1$ and $\epsilon \ll 1$. To leading order, we obtain the position of the critical point σ_c and show that the dynamics experience critical slowing down, meaning, in this context, that the correlation time of the noise $\delta\xi$ diverges as $\delta\sigma \to 0$. However, the scaling of ϵ with $\delta\sigma$, as well as the scaling of this relaxation timescale, are not captured by the expansion to that order, and to fully characterize the properties of the near-critical regime, one needs to go to the next-to-leading order. The resulting expansion is a mixed expansion in terms of $\delta\sigma$, ϵ and τ_c^{-1}, where τ_c is the typical long timescale over which near-critical fluctuations take place. Requiring that the resulting equation for the correlation function $\delta C(\tau)$ has a well-defined nontrivial solution imposes scaling relations between these three expansion parameters, finally allowing to derive the critical exponents defined in Sec. 2.

5.1 Leading-order expansion: position of the critical point and critical slowing down

Here we locate the position of the critical point, σ_c. A conventional way to do this from the DMFT equations, is to work in the phase where the dynamics converge to a fixed point,

and perturb the effective noise $\xi(t)$ by adding an infinitesimally small Gaussian white noise [5, 25]. The critical point is then identified by a diverging linear response of the dynamics to the perturbation. Here we follow a slightly different, but equivalent, route by working directly in the chaotic phase. Because fluctuations are already self-generated by the dynamics, there is no need to introduce an additional perturbing field. To proceed, we introduce the function

$$f(N,g) = N(1-g-N)+\lambda$$

so that the equation of motion for $\delta N(t)$ writes

$$\delta\dot{N} = \frac{1}{\epsilon} f\left(\bar{N}\left(\mu m_\infty - \sigma\bar{\xi}\right)+\epsilon\delta N, \mu m_\infty - \sigma\bar{\xi}\right) + \sigma\left(\bar{N}\left(\mu m_\infty - \sigma\bar{\xi}\right)+\epsilon\delta N\right)\delta\xi\,. \tag{37}$$

Using the condition $f\left(\bar{N}\left(\mu m_\infty - \sigma\bar{\xi}\right), \mu m_\infty - \sigma\bar{\xi}\right) = 0$, we can develop the nonlinearity is δN to first order and obtain, to leading order as $\delta\sigma \to 0$,

$$\delta\dot{N} = \partial_N f\left(\bar{N}\left(\mu m_c - \sigma_c\bar{\xi}\right), \mu m_c - \sigma_c\bar{\xi}\right)\delta N + \sigma_c\bar{N}\left(\mu m_c - \sigma_c\bar{\xi}\right)\delta\xi\,.$$

Note that, to this order, $\langle\delta N(t)\delta N(t+\tau)\rangle \to 0$ as $\tau\to\infty$ since δN is linear in $\delta\xi$. Therefore, in the Fourier domain, and making use of the self-consistency condition Eq. (35), we get

$$\left\langle|\delta N(\omega)|^2\right\rangle = \left\langle \frac{\sigma_c^2\bar{N}\left(\mu m_c - \sigma\bar{\xi}\right)^2}{\omega^2 + \partial_N f\left(\bar{N}\left(\mu m_c - \sigma\bar{\xi}\right), \mu m_c - \sigma_c\bar{\xi}\right)^2}\right\rangle_{w_c} \left\langle|\delta N(\omega)|^2\right\rangle\,. \tag{38}$$

Here the notation emphases that, to leading order, $\bar{\xi}$ is a Gaussian random variable sampled with variance w_c^2. The critical point is thus reached at σ_c which is such that

$$\left\langle \frac{\sigma_c^2\bar{N}\left(\mu m_c - \sigma\bar{\xi}\right)^2}{\partial_N f\left(\bar{N}\left(\mu m_c - \sigma\bar{\xi}\right), \mu m_c - \sigma_c\bar{\xi}\right)^2}\right\rangle_{w_c} = 1\,. \tag{39}$$

Indeed, for

$$\left\langle \frac{\sigma_c^2\bar{N}\left(\mu m_c - \sigma_c\bar{\xi}\right)^2}{\partial_N f\left(\bar{N}\left(\mu m_c - \sigma\bar{\xi}\right), \mu m_c - \sigma_c\bar{\xi}\right)^2}\right\rangle_{w_c} < 1\,.$$

the only solution to Eq. (38) would be $\left\langle|\delta N(\omega)|^2\right\rangle = 0$ for all ω. At $\sigma = \sigma_c$, non-trivial fluctuations are possible only for $\omega \to 0$, thus showing that the near-critical dynamics is characterized by a slow timescale that diverges as $\delta\sigma \to 0$. We have therefore identified the condition specifying the position of the critical point σ_c as given by Eq. (39), when supplemented by Eqs. (34, 36) with $\epsilon = 0$, meaning

$$m_c = \left\langle\bar{N}\left(\mu m_c - \sigma_c\bar{\xi}\right)\right\rangle_{w_c}\,, \tag{40}$$

and

$$w_c^2 = \left\langle\bar{N}\left(\mu m_c - \sigma_c\bar{\xi}\right)^2\right\rangle\,. \tag{41}$$

Numerically solving Eqs. (39,40,41) therefore allows one to obtain w_c, m_c and σ_c. Note that the critical condition Eq. (39) can be rewritten as

$$1 - \sigma_c^2\left\langle\bar{N}'\left(\mu m_c - \sigma_c\bar{\xi}\right)^2\right\rangle = 0\,. \tag{42}$$

This condition ensures that Eq. (35) is satisfied to leading order close to the critical point. For finite $\lambda > 0$, the result is that the transition line is pushed upwards, $\sigma_c > \sigma_c(\lambda = 0)$. In other words, migration helps to stabilize the fixed point, see Fig. 7 (a) and Eq. (54) below.

5.2 Beyond leading order: Expansion around the adiabatic approximation

In the previous section, we have shown that the fluctuations take place on timescales that diverge as the transition is approached, which we denote $\tau_c = \epsilon^{-r}$ with $r > 0$ a yet unknown critical exponent. To fully characterize the critical regime, that is the scaling of τ_c and ϵ with the distance $\delta\sigma$ from the critical point, one needs to go beyond leading order in the perturbative expansion. To proceed, it is therefore useful to expand the dynamics of $\delta N(t)$ around the adiabatic approximation δN_0 defined by the condition

$$\delta N_0(t) = \frac{1}{\epsilon}\left(\bar{N}\left(\mu m_\infty - \sigma\bar{\xi}\right) - \bar{N}\left(\mu m_\infty - \sigma\bar{\xi} - \sigma\epsilon\delta\xi(t)\right)\right), \tag{43}$$

which is obtained by setting $\dot{\delta N}$ to 0 in Eq. (37). The fluctuation timescale τ_c controls the deviations of $\delta N(t)$ from the adiabatic solution, allowing us to write $\delta N(t) = \delta N_0(t) + \tau_c^{-1}\delta N_1(t)$. After rescaling time by introducing $\tau = t/\tau_c$, the dynamics of $\delta N_1(\tau)$ is found to be governed by

$$\begin{aligned}\tau_c^{-1}\delta N_1'(\tau) = {}& \sigma\delta\xi'(\tau)\bar{N}'\left(\mu m_\infty - \sigma\bar{\xi} - \sigma\epsilon\delta\xi(t)\right) \\ & + \frac{\tau_c}{\epsilon} f\left(\bar{N}\left(\mu m_\infty - \sigma\bar{\xi}\right) + \epsilon\delta N_0(t) + \frac{\epsilon}{\tau_c}\delta N_1(t),\, \mu m_\infty - \sigma\bar{\xi} - \sigma\epsilon\delta\xi(t)\right),\end{aligned} \tag{44}$$

and the self-consistency condition on the correlation function becomes

$$\begin{aligned}&\langle\delta N_1(t)\delta N_1(t+\tau)\rangle + \tau_c\left(\langle\delta N_1(t)\delta N_0(t+\tau)\rangle + \langle\delta N_0(t)\delta N_1(t+\tau)\rangle\right) \\ &-\tau_c^2\left(\delta C(\tau) - \langle\delta N_0(t)\delta N_0(t+\tau)\rangle + \lim_{\tau\to\infty}\langle\delta N(t)\delta N(t+\tau)\rangle\right) = 0.\end{aligned} \tag{45}$$

To lowest order, $\delta N_1(t)$ is proportional to $\delta\xi'(\tau)$, as one finds

$$\delta N_1(\tau) = -\sigma_c\delta\xi'(\tau)\frac{\bar{N}'\left(\mu m_c - \sigma_c\bar{\xi}\right)^2}{\bar{N}\left(\mu m_c - \sigma_c\bar{\xi}\right)}. \tag{46}$$

The fact that $\delta N_1(\tau)$ depends on the derivative of the noise, unlike $\delta N_0(\tau)$ which is a function of $\delta\xi(\tau)$, is what allows to rephrase Eq. (45) as a differential equation for the correlation function $\delta C(\tau)$. To understand the scaling of ϵ and τ_c close to the critical point, it is instructive to inspect Eq. (45) term by term.

- The first term $\langle\delta N_1(t)\delta N_1(t+\tau)\rangle$ is of $O(1)$ and is proportional to $\delta C''(\tau)$, see Eq. (46), since $\left\langle\delta\xi'(t+\tau)\delta\xi'(t)\right\rangle = -\delta C''(\tau)$.
- The second term $\tau_c\left(\langle\delta N_1(t)\delta N_0(t+\tau)\rangle + \langle\delta N_0(t)\delta N_1(t+\tau)\rangle\right)$ seems to diverge as $O(\tau_c)$, but actually vanishes to that order. In fact, $\delta N_0(t) \sim \delta\xi(t)$ and $\delta N_1(t) \sim \delta\xi'(t)$ so that to leading order $\langle\delta N_1(t)\delta N_0(t+\tau)\rangle + \langle\delta N_0(t)\delta N_1(t+\tau)\rangle \sim \delta C'(\tau) + \delta C'(-\tau) = 0$. By going to the next order, we show below that this term yields an $O(1)$ contribution proportional to $\delta C''(\tau)$.
- The last term $\delta C(\tau) - \langle\delta N_0(t)\delta N_0(t+\tau)\rangle + \lim_{\tau\to\infty}\langle\delta N(t)\delta N(t+\tau)\rangle$ is a nonlinear function of $\delta C(\tau)$, without any derivative. A meaningful equation for $\delta C(\tau)$ can thus be obtained only if this term is combined with the first two terms proportional to $\delta C''(\tau)$, which thus requires it to scale as τ_c^{-2}. The critical condition in Eq. (42) ensures that it vanishes to order $O(1)$. Smaller corrections can then be obtained as an expansion in powers of $\delta\sigma$ and ϵ^2 (since the dynamics is invariant under $\epsilon \leftrightarrow -\epsilon$). Demanding that these corrections generate $O(1)$ contributions in Eq. (45) then imposes $\tau_c^{-1} \sim \epsilon \sim \sqrt{\delta\sigma}$, therefore yielding the value of the critical exponents $\beta = 1$ and $\zeta = 1/2$ introduced in Sec. 2.

The rest of the calculation, which involves expanding the three above mentioned terms to collect all contributions of $O(1)$, is straightforward but rather tedious. The detail of that expansion is presented in App. B. We eventually obtain a second-order differential equation for the correlation function $\delta C(\tau)$. After setting $\tau_c = \epsilon^{-1}$ and, to leading order, $\epsilon = \epsilon_0\sqrt{\delta\sigma}$, we find that the parameters of that equation explicitly depend on the yet unknown quantities ϵ_0, m_1 and w_1 where m_1 and w_1 are defined by the leading-order expansions $m - m_c = m_1\delta\sigma$ and $w - w_c = w_1\delta\sigma$. To close the system, and get ϵ_0, m_1 and w_1, three equations are needed. Two come from the self-consistency condition Eqs. (34, 36) while the third one comes from imposing that the differential equation satisfied by $\delta C(\tau)$ admits a solution such that $\delta C(0) = 0$, $\delta C(\infty) = 0$ and $\delta C'(0) = 0$.

5.3 A differential equation for the correlation function

The expansion presented in App. B shows that, to leading order as $\delta\sigma \to 0$,

$$\omega\delta C''(\tau) = -\kappa\delta C(\tau)^2 + \gamma\delta C(\tau), \tag{47}$$

where

$$\omega = \sigma_c^2 \left\langle \frac{\bar{N}'\left(\mu m_c - \sigma_c\bar{\xi}\right)^4}{\bar{N}\left(\mu m_c - \sigma_c\bar{\xi}\right)^2} \right\rangle_{w_c},$$

$$\kappa = \frac{\sigma_c^4}{2}\left\langle \bar{N}''\left(\mu m_c - \sigma_c\bar{\xi}\right)^2 \right\rangle_{w_c},$$

and

$$\begin{aligned}\gamma = \frac{1}{\epsilon_0^2}\Big[&-2\sigma_c\left\langle \bar{N}'\left(\mu m_c - \sigma_c\bar{\xi}\right)^2\right\rangle_{w_c} - 2\sigma_c^2\left\langle\left[\mu m_1 - \bar{\xi}\right]\bar{N}'\left(\mu m_c - \sigma_c\bar{\xi}\right)\bar{N}''\left(\mu m_c - \sigma_c\bar{\xi}\right)\right\rangle_{w_c}\\ &-\sigma_c^2 w_1\partial_w\left\langle \bar{N}'\left(\mu m_c - \sigma_c\bar{\xi}\right)^2\right\rangle_{w_c}\Big] - \sigma_c^2 w_1\partial_w\left\langle \bar{N}'\left(\mu m_c - \sigma_c\bar{\xi}\right)^2\right\rangle_{w_c}\\ &-\sigma_c^4\left\langle \bar{N}'\left(\mu m_c - \sigma_c\bar{\xi}\right)\bar{N}'''\left(\mu m_c - \sigma_c\bar{\xi}\right)\right\rangle_{w_c}.\end{aligned}$$

The parameters κ, γ and ω explicitly depend on ϵ_1, m_1 and w_1 which we haven't derived yet. However, for any given values of ϵ_1, m_1 and w_1, Eq. (47) can be seen as the classical equation of motion of a massive particle in a cubic potential. The conditions $\delta C_0(0) = 1$, $\delta C_0'(0) = 0$ and $\delta C_0(\infty) = 0$ then constrain the admissible value of γ to be

$$\gamma = \frac{2\kappa}{3}. \tag{48}$$

When this constraint is met, the equation can be solved exactly and its solution reads

$$\delta C_0(\tau) = 1 - \mathrm{Tanh}^2\left(\frac{\sqrt{\kappa}\tau}{6\sqrt{\omega}}\right). \tag{49}$$

Recalling that $\tau = \epsilon t$ and $\epsilon \sim \epsilon_0\sqrt{|\sigma - \sigma_c|}$, we recover the scaling form given in Eq. (8). The coefficient $\tau_c(\lambda, \mu)$ of Eq. (8) can be read from Eq. (49) as

$$\tau_c(\lambda, \mu) = \frac{6\sqrt{\omega}}{\epsilon_0\sqrt{\kappa}}. \tag{50}$$

Next we compute ϵ_0, m_1 and w_1, therefore leading to a closed-form expression for $\tau_c(\lambda, \mu)$. The result takes a simple form when $\lambda \ll 1$ and is reported in Sec. 5.6.

5.4 Obtaining the amplitude $Q_c(\lambda,\mu)$ and timescale $\tau_c(\lambda,\mu)$

So far, we have obtained the value of the critical exponents β and ζ as well as the scaling function governing the temporal decay of correlations. We have all the ingredients necessary to go further in characterizing the near-critical dynamics by deriving the amplitude $Q_c(\lambda,\mu)=\epsilon_0^2$ and timescale $\tau_c(\lambda,\mu)$, whose expression has been obtained in Eq. (50). This requires finding ϵ_0, m_1 and w_1. We can obtain two equations relating these three quantities by expanding the self-consistent DMFT equations for the variance of the frozen component of the noise and the mean population size–Eqs. (34) and (36) respectively–to order $O(\delta\sigma)$, by using the expansions of δN_0 and δN_1 presented in App. B. After some straightforward but tedious algebra, this leads to

$$\begin{aligned} &m_1\left(1-\mu\left\langle \bar{N}'\left(\mu m_c-\sigma_c\bar{\xi}\right)\right\rangle_{w_c}\right)-w_1\partial_w\left\langle \bar{N}\left(\mu m_c-\sigma_c\bar{\xi}\right)\right\rangle_{w_c}\\ &+\frac{\sigma_c^2}{2}\epsilon_0^2\left\langle \bar{N}''\left(\mu m_c-\sigma_c\bar{\xi}\right)\right\rangle=\left\langle \bar{\xi}\bar{N}'\left(\mu m_c-\sigma_c\bar{\xi}\right)\right\rangle_{w_c}, \end{aligned} \tag{51}$$

and

$$\begin{aligned} &-2\mu m_1\left\langle \bar{N}\left(\mu m_c-\sigma_c\bar{\xi}\right)\bar{N}'\left(\mu m_c-\sigma_c\bar{\xi}\right)^2\right\rangle_{w_c}+w_1\left(2w_c-\partial_w\left\langle \bar{N}\left(\mu m_c-\sigma_c\bar{\xi}\right)^2\right\rangle_{w_c}\right)\\ &+\sigma_c^2\epsilon_0^2\left\langle \bar{N}\left(\mu m_c-\sigma_c\bar{\xi}\right)\bar{N}''\left(\mu m_c-\sigma_c\bar{\xi}\right)-\frac{\sigma_c^2}{4}\bar{N}''\left(\mu m_c-\sigma_c\bar{\xi}\right)^2\right\rangle_{w_c}\\ &=-2\left\langle \bar{\xi}\bar{N}\left(\mu m_c-\sigma_c\bar{\xi}\right)\bar{N}'\left(\mu m_c-\sigma_c\bar{\xi}\right)^2\right\rangle_{w_c} \end{aligned} \tag{52}$$

The third equation necessary to solve for ϵ_0, m_1 and w_1 is provided by Eq. (48), which reads

$$\begin{aligned} &-2\mu\sigma_c^2 m_1\left\langle \bar{N}'\left(\mu m_c-\sigma_c\bar{\xi}\right)\bar{N}''\left(\mu m_c-\sigma_c\bar{\xi}\right)\right\rangle_{w_c}-\sigma_c^2 w_1\partial_w\left\langle \bar{N}'\left(\mu m_c-\sigma_c\bar{\xi}\right)^2\right\rangle_{w_c}\\ &-\epsilon_0^2\frac{\sigma_c^4}{3}\left\langle \bar{N}''\left(\mu m_c-\sigma_c\bar{\xi}\right)^2\right\rangle_{w_c}=\sigma_c^4\left\langle \bar{N}'\left(\mu m_c-\sigma_c\bar{\xi}\right)\bar{N}'''\left(\mu m_c-\sigma_c\bar{\xi}\right)\right\rangle_{w_c}\\ &+2\sigma_c\left\langle \bar{N}'\left(\mu m_c-\sigma_c\bar{\xi}\right)^2\right\rangle_{w_c}-2\sigma_c^2\left\langle \bar{\xi}\bar{N}'\left(\mu m_c-\sigma_c\bar{\xi}\right)\bar{N}''\left(\mu m_c-\sigma_c\bar{\xi}\right)\right\rangle_{w_c} \end{aligned} \tag{53}$$

The values of m_1, w_1 and ϵ_0, and from them those of $Q_c(\lambda,\mu)$ and $\tau_c(\lambda,\mu)$, can then be obtained by solving this linear system of equations. This allows to close the system of DMFT equations and characterize the dynamics to lowest order in the vicinity of the critical point.

5.5 Suppression of the chaotic phase at large λ

As we show now, these results indicate that the chaotic phase is suppressed for large values of λ, above a critical value $\lambda_c(\mu)$. In fact, for $\lambda>\lambda_c(\mu)$, we find that the collective dynamics in Eq. (1) directly experiences a transition from the fixed point phase when $\sigma<\sigma_c(\lambda,\mu)$ to a phase of unbounded growth when $\sigma>\sigma_c(\lambda,\mu)$, see Fig. 7. This phase of unbounded growth, in which population sizes blow up, was already investigated at low migration and was found to appear for large values of σ [6,31].

The critical parameter $\sigma_c(\lambda,\mu)$ which describes the onset of stability loss of the fixed point solution is still given by the solution of Eqs. (40, 41, 42). However, the set of linear equations prescribing the steady-state amplitude of the fluctuations close to the critical point $\epsilon_0^2=Q_c(\lambda,\mu)$, see Eqs. (51, 52, 53), admits a diverging solution at $\lambda=\lambda_c(\mu)$ and only (unphysical) negative solutions for $\lambda>\lambda_c(\mu)$, thus indicating the suppression of the chaotic phase.

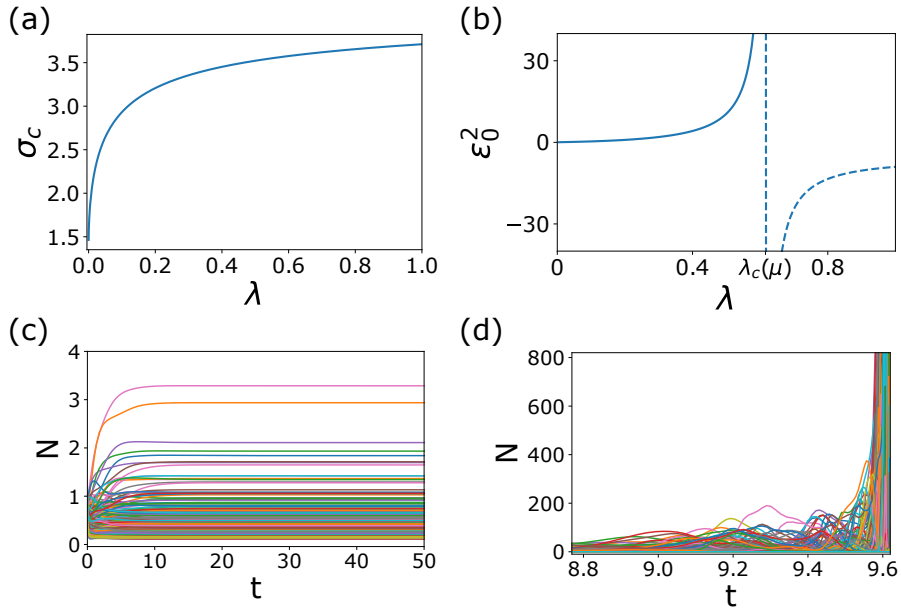

Figure 7: **Suppression of the chaotic phase at large migration rate. (a)** Onset of stability of the fixed point phase $\sigma_c(\lambda,\mu)$ as a function of λ for $\mu = 10$. **(b)** Amplitude of the chaotic fluctuations close to the transition $Q_c(\lambda,\mu) = \epsilon_0^2$ as a function of λ for $\mu = 10$ as predicted by the linear system of Eqs. (40, 41, 42). Above a certain value $\lambda > \lambda_c(\mu) \simeq 0.6$, the predicted value for $Q_c(\lambda,\mu)$ is negative, therefore signaling the suppression of the chaotic phase. **(c, d)** Many-body simulations of Eq. (1) with $S = 4000$ for $\mu = 10$ and $\lambda = 0.8 > \lambda_c(\mu)$. The loss of stability of the fixed phase is predicted to take place around $\sigma_c(\lambda,\mu) \simeq 0.65$. **(c)** Simulations at $\sigma = 0.6 < \sigma_c(\lambda,\mu)$. The dynamics converges to a fixed point. **(d)** Simulations at $\sigma = 0.7 > \sigma_c(\lambda,\mu)$. The dynamics enters a regime of unbounded growth of the population sizes.

5.6 Results when $\lambda \ll 1$

To connect these finite-λ results with the results obtained in the absence of migration and presented in Sec. 2, it is interesting to investigate the fate of our results when $0 < \lambda \ll 1$. By computing $Q_c(\lambda,\mu)$ and $\tau_c(\lambda,\mu)$ in that regime, we demonstrate the existence of the crossover discussed in Sec. 2.3. First, we need to investigate how the critical point σ_c, as well as the critical values m_c and w_c, are shifted in the presence of migration. By expanding Eqs. (40, 41, 42) at small $\lambda \ll 1$, we obtain that the deviations from the $\lambda = 0$ values scale as $\sqrt{\lambda}$ and that, to leading order,

$$\sigma_c \simeq \sqrt{2} + \frac{\sqrt{\lambda}\mu}{\sqrt{2}}, \tag{54}$$

showing that the position of the critical point now explicitly depends on μ and that a small amount of migration stabilizes the fixed point phase. We also obtain

$$w_c \simeq \frac{\sqrt{\pi}}{\mu}\left(1 + \frac{\sqrt{\lambda}}{4}(\pi(\mu+2) - 2\mu)\right), \tag{55}$$

and

$$m_c \simeq \frac{1}{\mu}\left(1 + \frac{\sqrt{\lambda}\pi}{2}\right). \tag{56}$$

Details about the perturbative expansion of Eqs. (40, 41, 42) leading to these expressions can be found in App. C. The results in Eqs. (54, 55, 56) can then be used in the linear system of Eqs. (51, 52, 53) that specify the value of ϵ_1, m_1 and w_1. After some lengthy but straightforward algebra, we obtain the leading order expression of these coefficients for $\lambda \ll 1$. Crucially, the amplitude of the fluctuations vanishes when $\lambda \to 0$ as we find

$$Q_c(\lambda,\mu) = \epsilon_0^2 \simeq \frac{16\sqrt{\lambda}}{\sqrt{2}\mu}, \tag{57}$$

and the timescale $\tau_c(\lambda,\mu)$ entering Eq. (8) diverges in that regime as we get

$$\tau_c(\lambda,\mu) \simeq \frac{\sqrt{3\mu\sqrt{2}}}{\lambda^{1/4}}. \tag{58}$$

Since $\sqrt{\lambda|\sigma-\sigma_c|} \ll |\sigma-\sigma_c|$ for $\lambda \ll \sqrt{\sigma-\sigma_c}$, these results suggest that the near-critical regime is controlled by another scaling limit when $\lambda \ll 1$ and $\sqrt{\lambda} \ll \sigma - \sqrt{2} \ll 1$, as discussed in Sec. 2.3. In fact, if that is the case, fluctuations whose amplitude and timescale behave as $|\sigma-\sqrt{2}|$ and $|\sigma-\sqrt{2}|^{-1/2}$, which are typical of the $\lambda \to 0^+$ universality class, are both much larger and faster than the ones identified here.

6 Conclusion

We have analytically described the Lotka-Volterra dynamics with many species and random interactions between them in the vicinity of the critical point separating the fixed phase to a phase of perpetual fluctuations. When approaching the critical point from the fluctuating phase, timescales are large and diverge at the transition (critical slowing down), while the size of the temporal fluctuations decreases continuously to zero. To characterize these two effects, we obtain the scaling behavior of the correlation function near the critical point. We identify two critical exponents β and ζ in the scaling theory, and calculate their values.

Our study highlights the effect of the migration rate λ on the critical dynamics. Depending on λ and the distance from the critical point $\sigma-\sigma_c$, we identify three different scaling regimes:

one for $\lambda = 0$, one for $\lambda > 0$ fixed, and one for $\lambda \to 0^+$, meaning that $\sqrt{\lambda} \ll \sigma - \sigma_c \ll 1$. This third regime $\sqrt{\lambda} \ll \sigma - \sigma_c$ is commonly probed in numerical investigations of the dynamics [7, 12]. The scaling behavior and the values of the exponents are different between these regimes.

This work raises a number of interesting questions for future study. One is the study of critical behavior when approaching the transition from the fixed point phase. In this phase there are no endogenous fluctuations at long times, but one can consider the relaxation close to the fixed point, and the response to external noise. Previous works have considered the linearized dynamics around the fixed point [5,12], looking only at the surviving species (those with $N > 0$ at the fixed point reached when $\lambda \to 0^+$). Yet the present and previous works [11, 13] highlight the importance of "species turnover" events where species abundances are exchanged between $O(\lambda)$ and $O(1)$ values, and this non-linear effect might be relevant also on the fixed point side of the transition. Another question of interest is the robustness of our results to changes in the model. We conjecture that the scenario outlined in this paper, of three universality classes corresponding to different regimes of migration, is quite generic, however with possible changes in the set of critical exponents. Indeed, as was shown in [11], the existence of a slow timescale when $\lambda \to 0^+$ extends to the Lotka-Volterra model with a level of symmetry in the interactions (presumably as long as the interaction matrix is not perfectly symmetric or antisymmetric). We also believe that the existence of a slow timescale is not specific to the Lotka-Volterra model with quadratic self-regulation. Dynamics described by $\dot{N}_i = N_i\left(1 - f(N_i) - \sum_j \alpha_{ij} N_j\right) + \lambda$ where $f(N_i)$ is monotonous and diverges at infinity, should also follow a similar behavior, as indicated by extending the mapping described in Sec. 4.1 to this case. Lastly, another interesting direction is the behavior at finite number of species S. The question of the width of the crossover region between the fixed-point phase and the chaotic or aging ones in finite size systems remains open, as is the behavior in this region; Simulations show that close to the transition limit cycles are sometimes reached, even with hundreds of variables.

Finally, it would be interesting to see if any of the critical behavior could be observed in experiments [26] or field studies. The main qualitative features–large timescales and small temporal fluctuations near the transition–are promising candidates.

Acknowledgements

We thank Anna Frishman and Yanay Tovi for useful discussions.

A Numerical methods

Here we detail the numerical procedures used to solve the DMFT equations. We start by giving detail about the $\lambda > 0$ case. We recall the DMFT equations

$$\dot{N}(t) = N(t)[1 - N(t) - \mu m(t) + \sigma\xi(t)] + \lambda\,, \tag{59}$$

with the conditions

$$m(t) = \langle N(t) \rangle\,, \tag{60}$$

and

$$C(t,t') = \left\langle \xi(t)\xi(t') \right\rangle = \left\langle N(t)N(t') \right\rangle\,, \tag{61}$$

These are self-consistent equations. The trajectory $N(t)$ depends on $\xi(t)$, which is sampled from the correlation function $C(t,t')$, and the function $m(t)$. Self-consistently, $C(t,t)$, $m(t)$ depend on the statistics of $N(t)$, see Eqs. (60, 61). This self-consistency is standard in DMFT formulations. We used a well-known numerical method to solve it [12, 34]. It starts with a guess for $C(t,t')$, $m(t)$, generates realizations of $\xi(t)$, and from that trajectories $N(t)$, which are then used to update $C(t,t')$, $m(t)$. The algorithm is summarized as follows:

1. We define a working time interval $[0,T]$ which we discretize at a sequence of intermediate times $\{t_i\}$. We also introduce a matrix $C_0(i,j)$ and a function $m_0(i)$ which serve as initial guesses for the searched correlation matrix $C(t_i,t_j)$ and mean population size $m(t_i)$.

2. We generate a matrix of random elements ξ_i^a, where $a = 1,\dots,N_{\text{traj}}$, with correlations $\left\langle \xi_i^a \xi_j^b \right\rangle = \delta_{ab} C_0(i,j)$, corresponding to a number N_{traj} of independent realizations of Gaussian processes with correlations $C_0(i,j)$.

3. We use these noise vectors to generate N_{traj} trajectories $\{N_i^a\}$ of population sizes following Eq. (59). Starting from some initial distribution of population sizes N_0^a, we approximate Eq. (59) by the recurrence relation defined by solving

$$\dot{N}^a(t) = N^a(t)\left[1 - N^a(t) - \mu m_0(i) + \sigma \xi_i^a\right] + \lambda$$

with initial condition $N^a(t_i) = N_i^a$ and set $N_{i+1}^a \equiv N^a(t_{i+1})$. This yields

$$N_{i+1}^a = \frac{\chi_{ia}^+ \left(N_i^a - \chi_{ia}^-\right) - \chi_{ia}^- \left(N_i^a - \chi_{ia}^+\right) \exp\left(-(\chi_{ia}^+ - \chi_{ia}^-)(t_{i+1} - t_i)\right)}{\left(N_i^a - \chi_{ia}^-\right) - \left(N_i^a - \chi_{ia}^+\right) \exp\left(-(\chi_{ia}^+ - \chi_{ia}^-)(t_{i+1} - t_i)\right)},$$

where

$$\chi_{ia}^{\pm} = \frac{1 - \mu m_0(i) + \sigma \xi_i^a \pm \sqrt{\left(1 - \mu m_0(i) + \sigma \xi_i^a\right)^2 + 4\lambda}}{2}.$$

Recall that, close to the transition, the noise varies slowly in time. This discretization is thus useful because it allows us to properly sample the population size trajectories using a time discretization binning that can be of arbitrary size, as long as $t_{i+1} - t_i$ is small compared to the correlation time of the noise.

4. We compute the corresponding empirical mean and correlation matrix as

$$m_{\text{emp}}(i) = \frac{1}{N_{\text{traj}}} \sum_a N_i^a$$

and

$$C_{\text{emp}}(i,j) = \frac{1}{N_{\text{traj}}} \sum_a N_i^a N_j^a .$$

We use these to update our guesses for the correlation function and mean population size using the update rule

$$m_1(i) = (1-e) m_0(i) + e m_{\text{emp}}(i),$$

$$C_1(i,j) = (1-e) C_0(i,j) + e C_{\text{emp}}(i,j),$$

where e is coined the injection fraction.

5. We repeat steps (2-4), replacing the initial guesses $C_0(i,j)$ and $m_0(i)$ by the updated correlation function and mean population size, until convergence.

In practice, at small $\delta\sigma = \sigma - \sigma_c$, the DMFT simulations were implemented with some theoretical knowledge of the expected outcome. In particular, we used $\tau_{\rm exp} = \tau_c(\lambda,\mu)/\sqrt{\delta\sigma}$, an expectation for the steady-state correlation time at finite $\delta\sigma$, to discretize the time interval. For each iteration, the noise $\xi(t)$ was sampled from the correlation function $C(t,t')$ over a time interval $t \in [0, 100\tau_{\rm exp}]$. The time interval was discretized in such a way that the bining dt becomes smaller and smaller with time, allowing a fast approach to and a precise sampling of the time-translation invariant steady state. Here we used $dt = 0.048\tau_{\rm exp}$ for $t \in [0, 60\tau_{\rm exp}]$, $dt = 0.0075\tau_{\rm exp}$ for $t \in [60\tau_{\rm exp}, 90\tau_{\rm exp}]$ and $dt = 0.0033\tau_{\rm exp}$ for $t \in [90\tau_{\rm exp}, 100\tau_{\rm exp}]$. For each realization of the discrete version of the dynamics in Eq. (10), the population size was initialized at a near fixed point value, so that $\left(N_0^a - 0.01\right)\left[1 - \left(N_0^a - 0.01\right) - \mu m(0) + \sigma\xi_0^a\right] + \lambda = 0$. For the first iteration, leveraging on our estimates for fluctuations and timescales, the initial guess for the correlation function $C_0(t,t')$ and mean $m_0(t)$ were the following: $m_0(t) = m_c$ and $C_0(t,t') = w_c^2 + \delta\sigma\exp(-|t-t'|/\tau_{\rm exp})$, which are small perturbations around their values at the critical point. We then used (i) 150 iterations with averaging over 1 000 trajectories and injection fraction 0.3 followed by (ii) 40 iterations with averaging over 10 000 realizations and injection fraction 0.3 followed by (iii) 400 iterations with averaging over 10 000 realizations and injection fraction 0.03 followed by (iv) 300 iterations with averaging over 10 000 realizations and injection fraction 0.003 followed by (v) 100 iterations with averaging over 100 000 realizations and injection fraction 0.003 and followed by (vi) 10 iterations with averaging over 1 000 000 realizations and injection fraction 0.003.

The simulations in rescaled time for the cases $\lambda \to 0^+$ and $\lambda = 0$, corresponding to the self-consistency equations (15, 16, 17, 18) and Eqs. (16, 17, 18, 32) respectively, used a very similar protocol (upon replacing t by s). For $\lambda = 0$, we chose $\tau_{\rm exp} = 2$, and we took $\tau_{\rm exp} = 2/\delta\sigma$ for $\lambda \to 0^+$. For the first iteration, we also chose $C(s,s') = w_c^2 + \delta\sigma^2\exp(-|s-s'|/\tau_{\rm exp})$. Lastly, the initial condition for the variable $z(s)$ at the beginning of each realization of the dynamics was $z(s) = -1$ if $1 - \mu m(0) + \sigma\xi(0) < 0$ and $z(s) = 0$ otherwise. The time integration of the dynamics for $z(s)$ in Eq. (15) and (32), both when $\lambda \to 0^+$ and $\lambda = 0$, was performed using a first order integration scheme taking into account the hard wall boundaries. For the $\lambda \to 0^+$ case, we used

$$z_{i+1}^a = \begin{cases} z_i^a + \left(1 - \mu m(i) + \sigma\xi_i^a\right)(t_{i+1} - t_i) & \text{if } -1 < z_i^a + \left(1 - \mu m(i) + \sigma\xi_i^a\right)(t_{i+1} - t_i) < 0 \\ 0 & \text{if } z_i^a + \left(1 - \mu m(i) + \sigma\xi_i^a\right)(t_{i+1} - t_i) > 0 \\ -1 & \text{if } z_i^a + \left(1 - \mu m(i) + \sigma\xi_i^a\right)(t_{i+1} - t_i) < -1 \end{cases},$$

and for the case $\lambda = 0$ we used

$$z_{i+1}^a = \begin{cases} z_i^a + \left(1 - \mu m(i) + \sigma\xi_i^a - z_i^a\right)(t_{i+1} - t_i) & \text{if } z_i^a + \left(1 - \mu m(i) + \sigma\xi_i^a - z_i^a\right)(t_{i+1} - t_i) < 0 \\ 0 & \text{if } z_i^a + \left(1 - \mu m(i) + \sigma\xi_i^a - z_i^a\right)(t_{i+1} - t_i) > 0 \end{cases}.$$

Note that close to the transition

$$(1 - \mu m + \sigma\xi) \sim \frac{\sqrt{2\pi}}{\mu},$$

since at the transition $\sigma = \sqrt{2}$, $1 - \mu m = 0$, and ξ has variance π/μ^2. For the values of $\delta\sigma$ and μ used in Fig. (4, 5), the time binning is such that $(1 - \mu m(i) + \sigma\xi_i^a)(t_{i+1} - t_i)$ remains small compared to 1, which is compatible with the use of a first order integration scheme.

B Perturbative expansion for $\lambda > 0$

This section aims at providing detail about the perturbative expansions of the three terms appearing in Eq. (45) used to obtain the results detailed in Sec. 5.3 of the main text.

B.0.1 Expanding $\langle \delta N_1(t)\delta N_1(t+\tau)\rangle$

To compute this term, one can use the leading order expression in Eq. 46. We immediately obtain

$$\langle \delta N_1(t)\delta N_1(t+\tau)\rangle = -\sigma_c^2 \left\langle \frac{\bar{N}'\left(\mu m_c - \sigma_c\bar{\xi}\right)^4}{\bar{N}\left(\mu m_c - \sigma_c\bar{\xi}\right)^2}\right\rangle_{w_c} \delta C''(\tau).$$

B.0.2 Expanding $\tau_c\left(\langle \delta N_1(t)\delta N_0(t+\tau)\rangle + \langle \delta N_0(t)\delta N_1(t+\tau)\rangle\right)$

To collect all terms to $O(1)$, we need to expand $\delta N_1(t)$ and $\delta N_0(t)$ up to order τ_c^{-1}. We use the result $\tau_c^{-1}\sim\epsilon$ that we will prove later on to expand δN_0 up to order $O(\epsilon)$. From Eq. (43), we get

$$\delta N_0(t) = \sigma\bar{N}'\left(\mu m_\infty - \sigma\bar{\xi}\right)\delta\xi(t) - \frac{\sigma^2}{2}\epsilon\delta\xi(t)^2\bar{N}''\left(\mu m_\infty - \sigma\bar{\xi} - \sigma\epsilon\delta\xi(t)\right) + O\left(\epsilon^2\right).$$

Accordingly, we get from Eq. (44)

$$\delta N_1(t) = -\sigma\delta\xi'(t)\frac{\bar{N}'\left(\mu m_\infty - \sigma\bar{\xi} - \sigma\epsilon\delta\xi(t)\right)^2}{\bar{N}\left(\mu m_\infty - \sigma\bar{\xi} - \sigma\epsilon\delta\xi(t)\right)} - \tau_c^{-1}\sigma\delta\xi''(t)\frac{\bar{N}'\left(\mu m_\infty - \sigma\bar{\xi} - \sigma\epsilon\delta\xi(t)\right)^3}{\bar{N}\left(\mu m_\infty - \sigma\bar{\xi} - \sigma\epsilon\delta\xi(t)\right)^2} + O\left(\epsilon\tau_c^{-1}\right).$$

Therefore we get to $O(1)$

$$\tau_c\left(\langle \delta N_1(t)\delta N_0(t+\tau)\rangle + \langle \delta N_0(t)\delta N_1(t+\tau)\rangle\right) = 2\sigma_c^2\left\langle \frac{\bar{N}'\left(\mu m_c - \sigma_c\bar{\xi}\right)^4}{\bar{N}\left(\mu m_c - \sigma_c\bar{\xi}\right)^2}\right\rangle_{w_c}\delta C''(\tau).$$

B.0.3 Expanding $\tau_c^2\left(\delta C(\tau) - \langle \delta N_0(t)\delta N_0(t+\tau)\rangle + \lim_{\tau\to\infty}\langle \delta N_0(t)\delta N_0(t+\tau)\rangle\right)$

To proceed, we need to expand first δN_0 to order $O\left(\epsilon^2\right)$. We get

$$\delta N_0(t) = \sigma\delta\xi(t)\bar{N}'\left(\mu m_\infty - \sigma\bar{\xi}\right) - \frac{\sigma^2}{2}\epsilon\delta\xi(t)^2\bar{N}''\left(\mu m_\infty - \sigma\bar{\xi}\right) + \frac{\sigma^3}{6}\epsilon^2\delta\xi(t)^3\bar{N}'''\left(\mu m_\infty - \sigma\bar{\xi}\right) + O\left(\epsilon^4\right).$$

Hence

$$\langle \delta N_0(t)\delta N_0(t+\tau)\rangle = \delta C(\tau)\left(\sigma^2\left\langle \bar{N}'\left(\mu m_\infty - \sigma\bar{\xi}\right)^2\right\rangle_w + \sigma_c^4\epsilon^2\left\langle \bar{N}'\left(\mu m_c - \sigma_c\bar{\xi}\right)\bar{N}'''\left(\mu m_c - \sigma_c\bar{\xi}\right)\right\rangle_{w_c}\right) + \frac{\sigma_c^4}{4}\epsilon^2\left\langle \bar{N}''\left(\mu m_c - \sigma_c\bar{\xi}\right)^2\right\rangle_{w_c}\left(2\delta C(\tau)^2 + 1\right) + O\left(\epsilon^4\right).$$

Therefore, we have

$$\begin{aligned}&\tau_c^2\left(\delta C(\tau) - \langle \delta N_0(t)\delta N_0(t+\tau)\rangle + \lim_{\tau\to\infty}\langle \delta N_0(t)\delta N_0(t+\tau)\rangle\right)\\ &= \tau_c^2\left(1 - \sigma^2\left\langle \bar{N}'\left(\mu m_\infty - \sigma\bar{\xi}\right)^2\right\rangle_w\right)\delta C(\tau) - \sigma_c^4\tau_c^2\epsilon^2\left\langle \bar{N}'\left(\mu m_c - \sigma_c\bar{\xi}\right)\bar{N}'''\left(\mu m_c - \sigma_c\bar{\xi}\right)\right\rangle_{w_c}\delta C(\tau)\\ &- \frac{\sigma_c^4}{2}\tau_c^2\epsilon^2\left\langle \bar{N}''\left(\mu m_c - \sigma_c\bar{\xi}\right)^2\right\rangle_{w_c}\delta C(\tau)^2.\end{aligned}$$

As claimed before, that the nonlinear term in δC yields an $O(1)$ contribution requires $\tau_c\sim\epsilon^{-1}$. In order to obtain the scaling of ϵ with $\delta\sigma$, we now need to expand the first term in powers

of $\delta\sigma$. From the criticality condition Eq. (42), we know that the leading order term in that expansion vanishes. Going to next order yields,

$$1-\sigma^2\left\langle \bar{N}'\left(\mu m_\infty-\sigma\bar{\xi}\right)^2\right\rangle_w=-2\sigma_c\delta\sigma\left\langle \bar{N}'\left(\mu m_c-\sigma_c\bar{\xi}\right)^2\right\rangle_{w_c}$$
$$-2\sigma_c^2\left\langle\left[\mu\delta m-\delta\sigma\bar{\xi}\right]\bar{N}'\left(\mu m_c-\sigma_c\bar{\xi}\right)\bar{N}''\left(\mu m_c-\sigma_c\bar{\xi}\right)\right\rangle_{w_c}-\sigma_c^2\delta w\partial_w\left\langle \bar{N}'\left(\mu m_c-\sigma_c\bar{\xi}\right)^2\right\rangle_{w_c}.$$

Additionally, to leading order, $\delta m=m_1\delta\sigma$ and $\delta w=w_1\delta\sigma$, so that we get

$$\tau_c^2\left(1-\sigma^2\left\langle \bar{N}'\left(\mu m_\infty-\sigma\bar{\xi}\right)^2\right\rangle_w\right)=\tau_c^2\delta\sigma\Big[-2\sigma_c\left\langle \bar{N}'\left(\mu m_c-\sigma_c\bar{\xi}\right)^2\right\rangle_{w_c}$$
$$-2\sigma_c^2\left\langle\left[\mu m_1-\bar{\xi}\right]\bar{N}'\left(\mu m_c-\sigma_c\bar{\xi}\right)\bar{N}''\left(\mu m_c-\sigma_c\bar{\xi}\right)\right\rangle_{w_c}$$
$$-\sigma_c^2 w_1\partial_w\left\langle \bar{N}'\left(\mu m_c-\sigma_c\bar{\xi}\right)^2\right\rangle_{w_c}\Big].$$

We can therefore conclude that $\tau_c^{-1}\sim\sqrt{\delta\sigma}$, from which one gets the critical exponents $\beta=1$ and $\zeta=1/2$ introduced in Sec. 2.

C Expansion when $\lambda\ll 1$

Here we present the expansion allowing us to obtain the shift in the critical values σ_c, w_c and m_c when $\lambda\ll 1$. The results are reported in Sec. 5.6 of the main text. When $\lambda=0$, we have $\sigma_c=\sqrt{2}$, $m_c=1/\mu$ and $w_c=\sqrt{\pi}/\mu$. At finite $0<\lambda\ll 1$, we write $m_c=1/\mu+\sqrt{\lambda}\delta m_c$ which allows us to expand Eq. (42) as

$$0=1-\frac{\sigma_c^2}{\sqrt{2\pi w_c^2}}\int_{-\infty}^{+\infty}\mathrm{d}\xi\exp\left(-\frac{\bar{\xi}^2}{2w_c^2}\right)\bar{N}'\left(\mu m_c-\sigma_c\bar{\xi}\right)^2,$$
$$\simeq 1-\frac{\sigma_c^2}{2}-\frac{\sigma_c^2\sqrt{\lambda}}{\sqrt{2\pi w_c^2}}\int_{-\infty}^{+\infty}\mathrm{d}\xi\exp\left(-\frac{\lambda\bar{\xi}^2}{2w_c^2}\right)\left[\frac{1}{4}\left(1+\frac{\sigma_c\bar{\xi}-\mu\delta m_c}{\sqrt{\left(\sigma_c\bar{\xi}-\mu\delta m_c\right)^2+4}}\right)^2-\Theta(\bar{\xi})\right],$$
$$\simeq 1-\frac{\sigma_c^2}{2}-\frac{\sqrt{2\lambda}\mu}{\pi}\int_{-\infty}^{+\infty}\mathrm{d}\bar{\xi}\left[\frac{1}{4}\left(1+\frac{\bar{\xi}}{\sqrt{\bar{\xi}^2+2}}\right)^2-\Theta(\xi+\mu\delta m_c/\sqrt{2})\right],$$
$$\simeq 1-\frac{\sigma_c^2}{2}+\frac{\sqrt{\lambda}\mu}{\pi}\left(\mu\delta m_c+\frac{\pi}{2}\right).$$

We therefore expand $\sigma_c=\sqrt{2}+\sqrt{\lambda}\delta\sigma_c$ and $w_c=\sqrt{\pi}/\mu+\sqrt{\lambda}\delta w_c$ to obtain to leading order

$$\delta\sigma_c=\frac{\mu}{\sqrt{2}\pi}\left(\mu\delta m_c+\frac{\pi}{2}\right). \tag{62}$$

We proceed similarly to expand Eq. (41)

$$
\begin{aligned}
0 &= w_c^2 - \frac{1}{\sqrt{2\pi w_c^2}} \int_{-\infty}^{+\infty} \mathrm{d}\bar{\xi} \exp\left(-\frac{\bar{\xi}^2}{2w_c^2}\right) \bar{N}\left(\mu m_c - \sigma_c \bar{\xi}\right)^2 , \\
&= w_c^2 - \frac{1}{\sqrt{2\pi w_c^2}} \int_{0}^{+\infty} \mathrm{d}\bar{\xi} \exp\left(-\frac{\bar{\xi}^2}{2w_c^2}\right) \left[\left(\sigma_c \bar{\xi} - \mu\sqrt{\lambda}\delta m_c\right)^2 + 2\lambda\right] \\
&- \frac{\lambda^{3/2}}{\sqrt{2\pi w_c^2}} \int_{-\infty}^{+\infty} \mathrm{d}\bar{\xi} \exp\left(-\frac{\lambda\bar{\xi}^2}{2w_c^2}\right) \left[\frac{1}{4}\left(\left(\sigma_c \bar{\xi} - \mu\delta m_c\right) + \sqrt{\left(\sigma_c \bar{\xi} - \mu\delta m_c\right)^2 + 4}\right)^2 \right. \\
&\left. - \left(\left(\sigma_c \bar{\xi} - \mu\delta m_c\right)^2 + 2\right)\Theta(\xi)\right] , \\
&\simeq w_c^2 - \frac{1}{\sqrt{2\pi w_c^2}} \int_{0}^{+\infty} \mathrm{d}\bar{\xi} \exp\left(-\frac{\bar{\xi}^2}{2w_c^2}\right) \left[\left(\sigma_c \bar{\xi} - \mu\sqrt{\lambda}\delta m_c\right)^2 + 2\lambda\right] + O\left(\lambda^{3/2}\right) , \\
&\simeq w_c^2 \left(1 - \frac{\sigma_c^2}{2}\right) + \sqrt{\frac{2\lambda}{\pi}} \mu\delta m_c w_c \sigma_c + O(\lambda) .
\end{aligned}
$$

Therefore, to leading order, we obtain

$$
\delta m_c = \frac{\pi}{\sqrt{2}\mu^2} \delta\sigma_c . \tag{63}
$$

Hence, we obtain from Eqs. (62, 63)

$$
\begin{aligned}
\delta\sigma_c &\simeq \frac{\mu}{\sqrt{2}} , \\
\delta m_c &\simeq \frac{\pi}{2\mu} .
\end{aligned}
$$

Lastly, δw_c can be obtained to leading order by expanding Eq. (40)

$$
\begin{aligned}
0 &= \frac{1}{\mu} + \sqrt{\lambda}\delta m_c - \frac{1}{\sqrt{2\pi w_c^2}} \int_{-\infty}^{+\infty} \mathrm{d}\xi \exp\left(-\frac{\bar{\xi}^2}{2w_c^2}\right) \bar{N}\left(\mu m_c - \sigma_c \bar{\xi}\right) \\
&= \frac{1}{\mu} + \sqrt{\lambda}\delta m_c - \frac{1}{\sqrt{2\pi w_c^2}} \int_{0}^{+\infty} \mathrm{d}\xi \exp\left(-\frac{\bar{\xi}^2}{2w_c^2}\right) \left(\sigma_c \bar{\xi} - \sqrt{\lambda}\mu\delta m_c\right) \\
&- \frac{\lambda}{\sqrt{2\pi w_c^2}} \int_{-\infty}^{+\infty} \mathrm{d}\xi \exp\left(-\frac{\lambda\bar{\xi}^2}{2w_c^2}\right) \left[\frac{\sqrt{4 + \left(\sigma_c \bar{\xi} + \mu\delta m_c\right)^2}}{2} - \sigma_c \bar{\xi}\,\Theta(\bar{\xi})\right] .
\end{aligned}
$$

Note that the last term scales as $O(\lambda \ln \lambda)$ since

$$
\frac{\sqrt{4 + \left(\sigma_c \bar{\xi} + \mu\delta m_c\right)^2}}{2} - \sigma_c \bar{\xi}\,\Theta(\bar{\xi}) =_{x\to\pm\infty} O\left(\frac{1}{x}\right) .
$$

Therefore, we obtain to leading order

$$
0 = \frac{1}{\mu} + \sqrt{\lambda}\delta m_c - \left(\frac{\sigma_c w_c}{\sqrt{2\pi}} - \mu\frac{\sqrt{\lambda}\delta m_c}{2}\right) + o\left(\sqrt{\lambda}\right) ,
$$

which yields

$$
\delta w_c \simeq \frac{\sqrt{\pi}}{4\mu} \left(\pi(\mu + 2) - 2\mu\right) .
$$

References

[1] E. H. van Nes, D. G. Pujoni, S. A. Shetty, G. Straatsma, W. M. de Vos and M. Scheffer, *A tiny fraction of all species forms most of nature: Rarity as a sticky state*, Proceedings of the National Academy of Sciences **121**(2), e2221791120 (2024).

[2] A. M. Martin-Platero, B. Cleary, K. Kauffman, S. P. Preheim, D. J. McGillicuddy, E. J. Alm and M. F. Polz, *High resolution time series reveals cohesive but short-lived communities in coastal plankton*, Nature communications **9**(1), 266 (2018).

[3] J. G. Caporaso, C. L. Lauber, E. K. Costello, D. Berg-Lyons, A. Gonzalez, J. Stombaugh, D. Knights, P. Gajer, J. Ravel, N. Fierer *et al.*, *Moving pictures of the human microbiome*, Genome biology **12**, 1 (2011).

[4] E. Benincà, J. Huisman, R. Heerkloss, K. D. Jöhnk, P. Branco, E. H. Van Nes, M. Scheffer and S. P. Ellner, *Chaos in a long-term experiment with a plankton community*, Nature **451**(7180), 822 (2008).

[5] M. Opper and S. Diederich, *Phase transition and 1/f noise in a game dynamical model*, Physical review letters **69**(10), 1616 (1992).

[6] G. Bunin, *Ecological communities with lotka-volterra dynamics*, Physical Review E **95**(4), 042414 (2017).

[7] I. Dalmedigos and G. Bunin, *Dynamical persistence in high-diversity resource-consumer communities*, PLoS computational biology **16**(10), e1008189 (2020).

[8] F. Roy, M. Barbier, G. Biroli and G. Bunin, *Complex interactions can create persistent fluctuations in high-diversity ecosystems*, PLoS computational biology **16**(5), e1007827 (2020).

[9] M. T. Pearce, A. Agarwala and D. S. Fisher, *Stabilization of extensive fine-scale diversity by ecologically driven spatiotemporal chaos*, Proceedings of the National Academy of Sciences **117**(25), 14572 (2020).

[10] E. Blumenthal, J. W. Rocks and P. Mehta, *Phase transition to chaos in complex ecosystems with nonreciprocal species-resource interactions*, Physical Review Letters **132**(12), 127401 (2024).

[11] T. Arnoulx de Pirey and G. Bunin, *Many-species ecological fluctuations as a jump process from the brink of extinction*, Physical Review X **14**(1), 011037 (2024).

[12] F. Roy, G. Biroli, G. Bunin and C. Cammarota, *Numerical implementation of dynamical mean field theory for disordered systems: Application to the lotka–volterra model of ecosystems*, Journal of Physics A: Mathematical and Theoretical **52**(48), 484001 (2019).

[13] T. Arnoulx de Pirey and G. Bunin, *Aging by near-extinctions in many-variable interacting populations*, Physical Review Letters **130**(9), 098401 (2023).

[14] J. Hofbauer and K. Sigmund, *Evolutionary games and population dynamics*, Cambridge university press (1998).

[15] H. Sompolinsky, A. Crisanti and H.-J. Sommers, *Chaos in random neural networks*, Physical review letters **61**(3), 259 (1988).

[16] T. Galla and J. D. Farmer, *Complex dynamics in learning complicated games*, Proceedings of the National Academy of Sciences **110**(4), 1232 (2013).

[17] T. Dessertaine, J. Moran, M. Benzaquen and J.-P. Bouchaud, *Out-of-equilibrium dynamics and excess volatility in firm networks*, Journal of Economic Dynamics and Control **138**, 104362 (2022).

[18] G. B. Arous, Y. V. Fyodorov and B. A. Khoruzhenko, *Counting equilibria of large complex systems by instability index*, Proceedings of the National Academy of Sciences **118**(34), e2023719118 (2021), doi:10.1073/pnas.2023719118.

[19] V. Ros, F. Roy, G. Biroli, G. Bunin and A. M. Turner, *Generalized lotka-volterra equations with random, nonreciprocal interactions: The typical number of equilibria*, Physical Review Letters **130**(25), 257401 (2023).

[20] G. Wainrib and J. Touboul, *Topological and dynamical complexity of random neural networks*, Phys. Rev. Lett. **110**, 118101 (2013), doi:10.1103/PhysRevLett.110.118101.

[21] J. D. O'Sullivan, J. C. D. Terry and A. G. Rossberg, *Intrinsic ecological dynamics drive biodiversity turnover in model metacommunities*, Nature Communications **12**(1), 3627 (2021).

[22] R. May and A. R. McLean, *Theoretical ecology: principles and applications*, Oxford University Press (2007).

[23] Y. Takeuchi, *Global dynamical properties of Lotka-Volterra systems*, World Scientific (1996).

[24] M. Barbier, J.-F. Arnoldi, G. Bunin and M. Loreau, *Generic assembly patterns in complex ecological communities*, Proceedings of the National Academy of Sciences **115**(9), 2156 (2018).

[25] T. Galla, *Dynamically evolved community size and stability of random lotka-volterra ecosystems (a)*, Europhysics Letters **123**(4), 48004 (2018).

[26] J. Hu, D. R. Amor, M. Barbier, G. Bunin and J. Gore, *Emergent phases of ecological diversity and dynamics mapped in microcosms*, Science **378**(6615), 85 (2022).

[27] G. Biroli, G. Bunin and C. Cammarota, *Marginally stable equilibria in critical ecosystems*, New Journal of Physics **20**(8), 083051 (2018).

[28] A. Altieri, F. Roy, C. Cammarota and G. Biroli, *Properties of equilibria and glassy phases of the random lotka-volterra model with demographic noise*, Physical Review Letters **126**(25), 258301 (2021).

[29] R. M. May and W. J. Leonard, *Nonlinear aspects of competition between three species*, SIAM journal on applied mathematics **29**(2), 243 (1975).

[30] J. Kadmon and H. Sompolinsky, *Transition to chaos in random neuronal networks*, Physical Review X **5**(4), 041030 (2015).

[31] J. W. Baron, T. J. Jewell, C. Ryder and T. Galla, *Breakdown of random-matrix universality in persistent lotka-volterra communities*, Physical Review Letters **130**(13), 137401 (2023).

[32] C. De Dominicis, *Dynamics as a substitute for replicas in systems with quenched random impurities*, Physical Review B **18**(9), 4913 (1978).

[33] J. Kadmon and H. Sompolinsky, *Transition to chaos in random neuronal networks*, Phys. Rev. X **5**, 041030 (2015), doi:10.1103/PhysRevX.5.041030.

[34] H. Eissfeller and M. Opper, *New method for studying the dynamics of disordered spin systems without finite-size effects*, Physical review letters **68**(13), 2094 (1992).